Palaeoenvironmental turnover across the Cenomanian-Turonian transition in Oued Bahloul, Tunisia: Foraminifera and geochemical proxies

Matías REOLID, Carlos Alberto SÁNCHEZ-QUIÑÓNEZ, Laia ALEGRET, Eustoquio MOLINA

Research Highlights:

Integrated analysis of foraminifera, geochemical proxies, $\delta^{13}C$ and $\delta^{18}O$. > Decreasing diversity and increasing of productivity and redox proxies during OAE2. > Habitat and trophic regimes of planktic foraminiferal fluctuations during OAE2. > Enhanced productivity and poor mixing waters favored eutrophication and OMZ expansion.

Palaeoenvironmental turnover across the Cenomanian-Turonian transition in Oued Bahloul, Tunisia: Foraminifera and geochemical proxies

Reolid, M.[1], Sánchez-Quiñónez, C.A.[2], Alegret, L.[3], Molina, E.[3]

1 Departamento de Geología, Universidad de Jaén, Campus Las Lagunillas sn, 23071 Jaén, Spain

2 Departamento de Geociencias, Universidad Nacional de Colombia, Bogotá, Carrera 30, nº 45-03, Colombia

3 Departamento de Ciencias de la Tierra e IUCA, Universidad de Zaragoza, Pedro Cerbuna 12, 50009 Zaragoza, Spain

* *Corresponding author:* mreolid@ujaen.es

ABSTRACT

The integrated analysis of foraminiferal assemblages, geochemical proxies, and stable isotopes in the Oued Bahloul section (Tunisia) allowed us to reconstruct the environmental turnover across the Cenomanian–Turonian boundary. An increase in palaeoproductivity proxies (P/Ti, U/Al, Sr/Al) and in $\delta^{13}C$ values, and a decrease in foraminiferal diversity and $\delta^{18}O$ values mark the beginning of the Oceanic Anoxic Event 2 (OAE2) at the *Rotalipora cushmani* and *Whiteinella archaeocretacea* biozones boundary. Eutrophic conditions at the seafloor and in the water column are evidenced by high proportions of buliminids and the replacement of planktic oligotrophic specialist *Rotalipora* by eutrophic opportunist *Hedbergella.* The enrichment in organic matter and redox sensitive elements, together with the abundance of low-oxygen tolerant benthic foraminifera, indicate dysoxic conditions in the deep-water column and at the

seafloor (higher U_{aut} than Mo_{aut}). Among planktic foraminifera, deep- and intermediate-dwellers disappear (*Rotalipora* and *Globigerinelloides*), and surface-dwellers proliferate (*Hedbergella*). The persistency of the poorly oxygenated conditions during the *W. archaeocretacea* Biozone locally produced euxinic conditions where Mo_{EF} and Mo_{aut} reach high values, diversity presents minimum values, and benthic foraminifera temporarily disappear. The maximum percentage of heterohelicids indicates a stratified water column with a well-developed oxygen minimum zone. Improved oxygen conditions returned in the upper part of the *W. archaeocretacea* Biozone and *Helvetoglobotruncana helvetica* Biozone, with a slow recovery of foraminiferal assemblages, decrease in eutrophic genera (*Heterohelix*) and increase in mesotrophic genera (*Whiteinella*). A gradual increase in $\delta^{18}O$ values suggests decreased temperatures in surface waters. The OAE2 has been attributed to global temperature changes and palaeoceanographic reorganization. The poor mixing of surface and deep waters and enhanced primary productivity related to global warming —associated with increasing continental weathering and nutrient runoff— may have favored the eutrophication of the ocean and the expansion of the oxygen minimum zone.

Keywords: trophic conditions, redox conditions, ecostratigraphy, foraminifera, OAE2, Cretaceous

1. Introduction

The Oceanic Anoxic Event 2 (OAE2), also called Bonarelli Event (e.g., Schlanger and Jenkyns, 1976; Arthur et al., 1990), is represented by the worldwide deposition of organic-rich facies close to the Cenomanian–Turonian (C-T) boundary. Two main hypotheses have been invoked to explain the deposition of organic-rich facies during the Cretaceous: (1) oceanic anoxia prevented the degradation of organic matter settling through the water column down to the seafloor by decreased oxygen supply to the deep ocean due to slower oceanic circulation (e.g. Erbacher et al., 2001; Tsandev and Slomp, 2009), or (2) enhanced surface water

productivity exceeded the oxygen availability for decaying organic matter at the seafloor (e.g. Sarmiento et al., 1988; Handoh and Lenton, 2003). The OAE2 has been related to palaeoceanographic and climatic changes including greenhouse warming (e.g. Huber et al., 2002; Norris et al., 2002; Bornemann et al., 2008; Tsandev and Slomp, 2009; Monteiro et al., 2012; Pogge von Strandmann et al., 2013), a sea-level transgression (Hallam, 1992), a perturbation of the carbon cycle (e.g. Kuypers et al., 2002; Erba, 2004; Pogge von Strandmann et al., 2013) and a probable massive magmatic episode (e.g. Kuroda et al., 2007; Turgeon and Creaser, 2008; Erba et al., 2013). The planktic foraminiferal turnover (Coccioni and Luciani, 2004; Caron et al., 2006) includes the disappearance of genus *Rotalipora* close to the OAE2 (e.g. Hart 1996, 1999; Nederbragt and Fiorentino, 1999; Keller et al., 2001; Coccioni and Luciani, 2004). Planktic foraminifera are sensitive to temperature, chemical and trophic conditions of the sea water (Caron, 1983; Caron and Homewood, 1983; Petrizzo, 2002; Gebhardt et al., 2004, 2010), and the ecostratigraphic analysis of their assemblages may be used to reconstruct palaeoceanographic and palaeoecological changes across the OAE2. In addition, the ecostratigraphic analysis of benthic foraminiferal assemblages is a useful tool to interpret fluctuations in oxygen and nutrient availability (e.g. Bernhard, 1986; Nagy, 1992; Jorissen et al., 1995; Van der Zwaan et al., 1999; Klein and Mutterlose, 2001; Reolid et al., 2008, 2012a, b). Some authors have interpreted an extinction event affecting benthic foraminiferal assemblages at the C-T boundary (e.g. Peryt and Lamolda, 1996; Kaiho, 1994, 1999; Peryt, 2004), yet there is no unanimity (Holbourn and Kuhnt, 2002).

The analysis of redox-sensitive trace elements (such as Co, Cr, Cu, Mo, and Ni, among others) has proven to be a powerful tool for interpreting redox conditions in oceans during anoxic events. These elements are less soluble under reducing conditions, resulting in synsedimentary enrichments under oxygen-depleted conditions (Wignall and Myers, 1988; Calvert and Pedersen, 1993; Jones and Manning, 1994; Powell et al., 2003; Gallego-Torres et al., 2007; Reolid et al., 2012a, b). Geochemical proxies have also been successfully applied to interpret palaeoproductivity, the most extensively used being Ba/Al, Sr/Al, Ca/Al and P/Ti

ratios (e.g., Turgeon and Brumsack, 2006; Gallego-Torres et al., 2007; Robertson and Filippelli, 2008; Sun et al., 2008; Reolid and Martínez-Ruiz, 2012; Reolid et al., 2012a, b). The total organic carbon (TOC) has also been employed as an indirect palaeoproductivity proxy (e.g., Gupta and Kawahata, 2006; Su et al., 2008), although enhanced TOC contents may result from low bottom-water ventilation and oxygen depletion.

The aim of this work is to integrate planktic and benthic foraminiferal assemblages and geochemical proxies to determine the palaeoenvironmental turnover across the OAE2 in the Oued Bahloul section, Tunisia. The OAE2 and the C-T transition are recorded in the Bahloul Formation, where numerous studies on microfacies, planktic foraminifera, organic matter and stable isotopes have been carried out (e.g. Caron et al., 1999, 2006; Accarie et al., 2000; Amédro et al., 2005; Zagrarni et al., 2008; Negra et al., 2011; Soua et al., 2011; for recent works). Here we present the first integrated analysis of foraminiferal assemblages and geochemical proxies across the C–T transition at Oued Bahloul.

2. Geological setting and the Oued Bahloul section

The Cretaceous palaeogeography of Tunisia consists of three main domains: the Saharan Platform in the South, the Central Tunisian Platform, and the Tunisian Basin in the North (Burollet and Busson, 1983). The Central Tunisian Platform was mainly occupied by outer shelf facies rich in planktic foraminifera during the C-T interval. The Bahloul Formation is a widespread wedge that ranges from 23 m thick in the North to 2 m thick in the South, upon the Cenomanian Central Tunisian Platform (Saïdi et al., 1997; Scott, 2003; Robaszynski et al., 2010; Zaghbib-Turki and Soua, 2013; Fig. 1).

The Oued Bahloul section was proposed by Burollet (1956) as the type locality of the Bahloul Formation. This outcrop presents the best sedimentary record of the OAE2 in the southern margin of the Tethys (Robaszynski et al., 1993; Caron et al., 2006). The OAE2 is marked by a strong positive shift in $\delta^{13}C$ in bulk carbonate and an increase in organic matter

content in the Bahloul Formation (Accarie et al., 1996; Nederbragt and Fiorentino, 1999). The studied interval is 47 m thick and includes the uppermost 5 m of the Fahdène Formation, the Bahloul Formation (29 m thick) and the lowermost 13 m of the Kef Formation (Fig. 1). The Fahdène Formation consists of an alternation of grey-greenish marls and light-coloured limestones. The Bahloul Formation is divided into two members: lower Pre-Bahloul Member and upper Bahloul *s*. *str*. Member (Fig. 1). In turn, the Pre-Bahloul Member is 3.4 m thick and its lower boundary with the Fahdène Formation is sharp and erosive. The first level (0.5 m thick) is a sandy micro-conglomeratic limestone that contains phosphatic black pebbles and quartz grains with well-developed graded bedding. The overlying bed is a bioclastic-rich calcarenite. The upper part of the Pre-Bahloul Member consists of marls with a decreasing content of quartz and bioclasts.

The Bahloul *s*. *str*. Member, in this work Bahloul Member, is composed of an alternation of 2 to 5 cm thick, bedded black limestones with thin parallel lamination, and grey marls. Different calcareous packages (50 cm thick) may be recognized where thin black limestones dominate versus intervals with dominance of grey marls. The lamination of the black limestones consists of clear laminae with abundant planktic foraminifera, and black laminae with abundant pellets embedded in a dark matrix with common radiolaria, benthic foraminifera (buliminids) and planktic foraminifera. The vertical transition from laminated black limestones to grey marls is gradual, but the transition from grey marls to black laminated limestones is abrupt. The top of the Bahloul Formation corresponds to densely bioturbated grey marls, and is locally overlain by a thin limestone layer rich in ammonoid moulds with phosphate and glauconite grains (Caron et al., 2006; Zagrarni et al., 2008). The overlying Annaba Member of the Kef Formation consists of grey marls with interlayered marly-limestones.

Robaszynski et al. (1990, 1993) located a sequence boundary at the top of Fahdène Formation, at the base of a channel-fill limestone bed (Ce SB5 *s*. Hardenbol et al., 1998). These authors situated the transgressive contact (Ce TS5) at the top of a thicker limestone bed, and the maximum flooding surface between the black laminated limestones of the Bahloul Formation

and the marls of the Kef Formation.

3. Material and methods

Foraminiferal and geochemical analyses were conducted across the upper Cenomanian-lower Turonian at Oued Bahloul section. A total of 25 sampling levels were selected from this 47 m thick limestone and marly-limestone succession (Fig. 1). Micropalaeontological samples were disaggregated in water with diluted H_2O_2, washed through a 63 μm sieve, and dried at 50ºC. More endurated limestones were immersed in acetic acid (80%) during 1 h to 4 h, depending on the carbonate content, then washed through a 63 μm sieve, and dried at 50ºC.

Quantitative studies (Tables 1 and 2) were based on representative splits (using a modified Otto microsplitter) of over 300 specimens of benthic foraminifera larger than 63 μm and 300 specimens of planktic foraminifera larger than 100 μm per sample. The remaining residue was scanned for rare species. Planktic foraminiferal taxa (Fig. 2) were also allocated to biserial (*Heterohelix*), triserial (*Guembelitria*), planispiral (*Globigerinelloides*), and trochospiral morphogroups (Table 3). The latter include strongly keeled (*Dicarinella*, *Rotalipora, Thalmanninella*), weakly keeled (*Anaticinella*, *Helvetoglobotruncana*, *Praeglobotruncana*) and unkeeled (*Hedbergella*, *Schackoina, Whiteinella*) forms (Table 3). Changes in depth stratification of the water column and trophic structure, temperature and salinity are the main factors controlling the composition of planktic foraminiferal assemblages. The stratification and richness of nutrients in the water column is narrowly related to productivity and the behavior of the planktic foraminifera. In this sense, opportunists (r-strategists) flourish in eutrophic waters whereas specialists (K-strategists) proliferate in oligotrophic waters (Valentine, 1973). Depth stratification favored differentiation of biotic and abiotic environmental features providing distinct ecological niches and minimizing the competition among species (Hemleben et al., 1989). Based on morphotype analyses (e.g. Corliss, 1985; Jones and Charnock, 1985; Corliss and Chen, 1988), benthic foraminiferal taxa (Fig. 3) were allocated to infaunal, epifaunal, and

epifaunal/infaunal morphogroups. In general, benthic foraminifera with trochospiral, planoconvex or biconvex tests are inferred to have had an epifaunal mode of life, living at the sediment surface or in its upper few centimetres, while infaunal foraminifera have cylindrical or flattened tapered, spherical, globular unilocular or elongated multilocular tests, and live in the deeper layers of the sediment (Corliss, 1991; Reolid et al., 2008). Simple diversity (number of species) and the Fisher-α diversity index (e.g. Murray, 1991) were calculated separately for benthic and planktic foraminiferal assemblages.

Whole-rock analyses of major elements were carried out in 25 samples using X-ray fluorescence (XRF) in a Philips PW 1040/10 spectrometer. The content of trace elements was determined using an inductively coupled plasma-mass spectrometer (ICP-MS Perkin Elmer Sciex-Elan 5000) at the Centro de Instrumentación Científica (CIC, Universidad de Granada). Instrumental error was ± 2% and ± 5% for respective elemental concentrations of 50 ppm and 5 ppm.

The contents in C, N and S, as well as the total organic carbon (TOC) content, were analysed analyzed with an Elemental Analyzer LECO CNS-TruSpec and an Inorganic Carbon Analyzer CM5240 UIC in the laboratories of the Centro Andaluz de Medio Ambiente (CEAMA, Granada). Total organic carbon was obtained as the difference between total carbon and total inorganic carbon; it was measured in mg and calculated as percentage of sample weight.

For $\delta^{13}C$ and $\delta^{18}O$ analyses, and after roasting, the samples were reacted at 73ºC in an automated carbonate reaction system (Kiel-IV) coupled directly to the inlet of a Finnigan MAT 253 gas ratio mass spectrometer at the Laboratory of Stable Isotopes of the University of Michigan. Isotopic ratios were corrected for ^{17}O contribution and are reported in per mil notation relative to the VPDB standard. Values were calibrated using NBS 19 as the primary standard, and analytical precision was monitored by daily analyses of NBS powdered carbonate standards. The measured precision was maintained above 0.02‰ for $\delta^{13}C$ and $\delta^{18}O$.

188 In order to compare trace-element proportions in samples with varying carbonate and
189 clay contents, trace-element concentrations were normalized to aluminium content (Calvert and
190 Pedersen, 1993). This technique avoids any lithological effects on trace or major element
191 concentrations, assuming that Al content in sediments is heightened by alumino-silicates (e.g.,
192 Calvert, 1990). The study of palaeoproductivity was carried out applying a set of proxies (Sr/Al,
193 U/Al and P/Ti). To analyzse palaeo-oxygenation, diverse redox proxies evaluating the relative
194 increase of redox sensitive elements (Co/Al, Cr/Al, Cu/Al, Mo/Al, Ni/Al, and Th/Al) were
195 applied throughout the section. Distinct enrichment factors (Mo and U), applied according to
196 Zhou et al. (2012) and Tribovillard et al. (2012), included $Mo_{EF}= [Mo/Al]_{sample}/[Mo/Al]_{PAAS}$ and
197 $U_{EF}= [U/Al]_{sample}/[U/Al]_{PAAS.}$ The authigenic values of U and Mo were also calculated according
198 to Zhou et al. (2012), as $Mo_{aut}=[Mo]_{sample}-[Mo]_{PAAS}/[Al]_{PAAS}*[Al]_{simple}$, $U_{aut}=[U]_{sample}-$
199 $[U]_{PAAS}/[Al]_{PAAS}*[Al]_{simple}$.
200
201 **4. Results**
202
203 *4.1. Planktic foraminifera and biostratigraphy*
204
205 Planktic foraminifera dominate the assemblages in the Fahdène Formation (Fig. 4),
206 where the P/B ratio is high (up to 93%). P/B values gradually decrease from the uppermost part
207 of this formation towards the Bahloul Formation, with values commonly <30%, then gradually
208 increase up to 98% towards the middle part of the Bahloul Formation (metre 17), remaining low
209 (<30%) throughout the rest of the section and slightly increasing (up to 57%) in the lower part
210 of the Kef Formation (Fig. 4).
211 A total of 13 genera and 31 species of planktic foraminifera were identified at Oued
212 Bahloul (Fig. 2, Appendix 1). The species distribution allowed us to identify the *Rotalipora*
213 *cushmani, Whiteinella archaeocretacea* and *Helvetoglobotruncana helvetica* biozones (Fig. 5).
214 The upper Cenomanian *R. cushmani* Biozone corresponds to the lower part of the studied

interval, and is mostly represented by the Fahdène Formation (Fig. 5). This interval contains abundant keeled trochospiral forms, such as *Rotalipora cushmani*, *Thalmanninella greenhornensis*, *Thalmannninella brotzeni*, *Rotalipora monsalvensis* and *Anaticinella multiloculata* (with a poorly developed keel). The *W. archaeocretacea* Biozone is 28 m thick, and it includes the uppermost 50 cm of the Fahdène Formation and the Bahloul Formation, containing the Cenomanian-Turonian boundary. This biozone is characterised by common biserial forms such as *Heterohelix reussi* and unkeeled trochospiral forms such as *Whiteinella archaeocretacea, Whiteinella aprica*, *Hedbergella planispira* and *Hedbergella delrioensis*. The *H. helvetica* Biozone (lower Turonian) is represented in the uppermost 1.2 m of the Bahloul Formation and in the Kef Formation. This biozone is characterised by the species *Helvetoglobotruncana helvetica*, *Dicarinella imbricata, Shackoina bicornis* and *Whiteinella paradubia*.

The correlation of the planktic foraminiferal and ammonite (Caron et al., 1999, 2006; Amédro et al., 2005) biozones is shown in Fig. 1C. The record of *Pseudocalycoceras angolaense* in the Pre-Bahloul Member and lowermost 3 m of the Bahloul Member indicates the *Metoicoceras geslinianum* Biozone (Cenomanian). The record of *Pseudaspidoceras pseudonodosoides* in the Bahloul Formation (12 to 29 m) indicates a late Cenomanian age (*P. pseudonodosoides* Biozone), and the record of *Watinoceras* and *Fagesia* in the topmost Bahloul Formation indicates early Turonian age (*Watinoceras* Biozone) (Fig. 1C). The base of the Kef Formation is lower Turonian in age: the *Pseudaspidoceras flexuosum* Biozone has been inferred by correlation with other sections (Accarie et al., 2000), and the *Thomasites rollandi* Biozone is indicated by the record of *Thomasites* sp. (Caron et al., 2006).

Diversity of planktic foraminiferal assemblages (Fig. 4) shows a decreasing trend from the Fahdène Formation towards the lower half of the Bahloul Formation (uppermost part of the *R. cushmani* Biozone and lower part of the *W. archaeocretacea* Biozone). Some taxa went extinct (e.g., *Globigerinelloides ultramicrus, Thalmanninella brotzeni, T. greenhornensis, Rotalipora cushmani, R. monsalvensis*), and others (e.g. *Anaticinella multicostata, Dicarinella*

242 spp., *Globigerinelloides bentonensis*, *Schackoina* spp.) temporarily disappeared across this
243 interval and reappeared within the upper half of the *W. archaeocretacea* Biozone. Assemblages
244 diversified towards the top of the section, where diversity values are similar to those in the
245 Fahdène Formation (Fig. 4).
246 Assemblages from the lowermost part of the section include common to abundant
247 planispiral (*Globigerinelloides bentonensis*), trochospiral (*Hedbergella delrioensis, H.*
248 *planispira, H. simplex*) and biserial forms (*Heterohelix reussi*) (Fig. 5). Right at the base of the
249 *Whiteinella archaeocretacea* Biozone, the abundance of *H. delrioensis* increases up to 67% of
250 the assemblage (metre 7), and minor quantitative peaks in *Thalmanninella brotzeni* and
251 *Whiteinella aprica* are observed (Fig. 5). Assemblages from the lower half of the Bahloul
252 Formation are strongly dominated by *Heterohelix reussi* (up to 78% of the assemblage), whose
253 relative abundance decreases towards the upper half of this formation, where trochospiral taxa
254 (e.g., *W. archaeocretacea, W. aprica*, *W. baltica*) become common to abundant. Assemblages
255 from the Kef Formation are similar to those from the upper Bahloul Formation, but they contain
256 higher percentages of triserial (*Guembelitria cenomama*), trochospiral (*Hedbergella delrioensis*)
257 and biserial morphogroups (e.g, *Globoheterohelix paraglobulosa*). A 5 m thick interval in the
258 Kef Formation (metres 37–42) is strongly dominated by *W. aprica,* which is rapidly replaced by
259 *Heterohelix reussi* in the uppermost part of the studied section (Fig. 5).
260
261 *4.2. Benthic foraminifera*
262
263 Among benthic foraminifera, calcareous taxa dominate over agglutinated ones. A total
264 of 45 genera and 70 species were recorded throughout the Oued Bahloul section (Appendix 2).
265 *Neobulimina*, *Gavelinella*, *Praebulimina*, *Tappanina*, and *Lenticulina* are the most common
266 genera. *Trochammina*, *Gyroidinoides* and *Laevidentalina* are locally abundant (Fig. 6).
267 Changes in diversity of benthic foraminiferal assemblages are similar to those of
268 planktic assemblages, showing a decreasing trend from the Fahdéne Formation to the middle

part of the Bahloul Formation, with minimum values in metres 10–17, and gradual recovery above this interval towards the top of the section (Fig. 4). Sample 17 (Bahloul Formation) is barren of benthic foraminifera (Fig. 6), and very few specimens were found in samples OB-28, OB-30, OB-37, OB-38 and OB-40; thus the benthic foraminiferal counts are not considered as representative in these samples. While planktic foraminiferal assemblages from the uppermost part of the studied section (upper part of *W. archaeocretacea* Biozone and *H. helvetica* Biozone) reach diversity values similar to those in the Fahdéne Formation, the diversity of benthic foraminifera does not fully recover and is significantly lower at the top of the section.

Benthic foraminiferal assemblages from the lowermost part of the section are diverse and dominated by epifaunal trochospiral forms (e.g., *Gavelinella flandrini, Gyroidinoides globosus* and *Gyroidinoides lenticulus*). Spherical (*Trochammina globolaevigata*) and cylindrical tapered morphogroups (*Praebulimina reussi* and *Laevidentalina* spp.) are also common. The relative abundance of *Gavelinella* spp. significantly increases to the top of Pre-Bahloul Member (Fig. 6), and assemblages are clearly dominated by *Gavelinella* spp., *Lenticulina gaultina*, and abundant *Globorotalites* spp. (Fig. 6).

The boundary between the Pre-Bahloul Member and the Bahloul Member (lower part of the *W. archaeocretacea* Biozone) is characterised by an abrupt decrease in the relative abundance of *Gavelinella* and *Lenticulina,* the disappearance of such taxa as *Trochammina* sp., *Globorotalites* spp. and *Lingulogavelinella frankei*, and the temporary disappearance of *Laevidentalina* spp., *Laevidentalina gaultina* and *Lenticulina subgaultina* (Lazarus taxa). This boundary marks a clear change in benthic assemblages, from epifauna-dominated assemblages in the lower part of the section to infauna-dominated assemblages in the rest of the studied section. Low-diversity assemblages from the lower half of the Bahloul Member are clearly dominated by *Neobulimina albertensis* (up to 81% of the assemblages), with a minor contribution of *Tappanina laciniosa* and *Coryphostoma* spp. The upper part of this member contains more diversified assemblages, with abundant *Neobulimina albertensis* and *T. laciniosa*,

295 common *Laevidentalina* spp., and new taxa such as *Gavelinella rochardensis* and *Bolivina* sp.
296 (Fig. 6).

297 The lowermost 2.5 m of the *H. helvetica* Biozone are characterised by the disappearance
298 of *Astacolus* spp. and *Dorothia* spp. The Annaba Formation (*H. helvetica* Biozone) contains
299 highly variable percentages of *Neobulimina albertensis* and quantitative peaks of infaunal
300 (*Lenticulina subgaultina*, *Bolivina* spp.) and some epifaunal taxa (*Gavelinella* spp.,
301 *Gyroidinoides lenticulus*).

302

303 *4.3. Geochemistry*

304

305 *4.3.1. Redox proxies*

306 The stratigraphic distribution throughout the succession of the analysed ratios shows
307 three intervals with main changes: a) the base of the *W. archaeocretacea* Biozone, b) the middle
308 part of the *W. archaeocretacea* Biozone, and c) the *W. archaeocretacea*/*H. helvetica* biozone
309 boundary.

310 The lowermost part of the section (*R. cushmani* Biozone) is characterised by decreasing
311 Co/Al, Ni/Al and Th/Al ratios, followed by a sudden increase in all the studied proxies in the
312 Pre-Bahloul Member (base of *W. archaeocretacea* Biozone, Fig. 7). The Mo_{EF}, $Mo_{aut.}$, U_{EF} and
313 $U_{aut.}$ ratios also increase in the Pre-Bahloul Member, with a dramatic increase in U proxies in
314 the topmost Fahdène Formation (*R. cushmani*/*W. archaeocretacea* biozone boundary),
315 immediately preceding the peaks of all other proxies. The U_{EF} values reach 8.08, which is very
316 relevant (Fig. 7). According to Tribovillard et al. (2012), values of elemental enrichment factor
317 > 3 are considerable and > 10 is considered as a strong enrichment.

318 An increase in the Cr/Al ratio and in Mo_{EF} and Mo_{aut} values, and a minor increase in
319 Cu/Al, Ni/Al, U_{EF} and U_{aut} are recorded in sample OB-17 (metre 17, middle part of the *W.*
320 *archaeocretacea* Biozone), which is barren of benthic foraminifera (Fig. 7).

The Th/Al ratio remains constant throughout the rest of the section, while the other proxies increase towards the top of the Bahloul Formation (*W. archaeocretacea*/*H. helvetica* biozone boundary), where new peaks in Co/Al, Cr/Al, Cu/Al, Ni/Al and Mo_{EF} and minor increases in Th/Al, $Mo_{aut.}$, U_{EF} and U_{aut} are observed (Fig. 7). Towards the top of the section (Annaba Member), the selected ratios return to the original values recorded in the lowermost part of the section (Fahdène Formation).

4.3.2. Palaeoproductivity proxies and TOC

In contrast to redox proxies, the selected palaeoproductivity proxies and TOC only show prominent changes in the Pre-Bahloul Formation (base of the *W. archaeocretacea* Biozone; Fig. 8). The U/Al and P/Ti ratios increase coinciding with the first peak in redox proxies, whereas TOC reaches the maximum values (2.8 wt.%) 1 m above the U/Al and P/Ti peaks. TOC values fluctuate throughout the rest of the section but never exceed the high values recorded at the top of the Pre-Bahloul Formation. The Sr/Al ratio and TOC values (2.1 wt.%) are higher in the *W. archaeocretacea*/*H. helvetica* biozone boundary than in the other biozones. Apart from decreased TOC and Sr/Al values in the lower half of the Annaba Member, palaeoproductivity proxies remain relatively stable up to the top of the section.

4.3.3. $\delta^{13}C$ and $\delta^{18}O$

Bulk rock $\delta^{13}C$ values obtained in this study have been compared to previous results by Caron et al. (2006) and Zagrarni et al. (2008), and show similar trends (Fig. 9). A 2‰ increase (from 1.83 – 3.76‰) in $\delta^{13}C$ is recorded at the transition from the Pre-Bahloul Member to the Bahloul Member (lower part of the *W. archaeocretacea* Biozone). A marked increase in $\delta^{13}C$ values is a typical feature of the OAE2 (e.g. Scholle and Arthur, 1980; Schlanger et al., 1987). $\delta^{13}C$ values remain high throughout most of the *W. archaeocretacea* Biozone (mean value 3.09‰), and decrease in its uppermost 5 m. The $\delta^{13}C$ mean value in the *H. helvetica* Biozone (base of the Annaba Member) is 2.30‰.

348 The $\delta^{18}O$ values gradually decrease from the Fahdène Formation to the Bahloul Member
349 (from -4.54 to -5.31‰), and remain low (mean value -5.39‰) throughout the rest of the Bahloul
350 Formation, progressively increasing in the Annaba Member (mean value -4.55‰).
351
352 **5. Palaeoenvironmental interpretation**
353
354 *5.1. Top of the Fahdène Formation and Pre-Bahloul Member*
355
356 Analysis of redox conditions in the water column and at the seafloor is based on redox-
357 sensitive trace elements (Co, Cr, Cu, Mo, Ni, U, and Th), which tend to co-precipitate with
358 sulfides (mainly pyrite) and are usually not remobilised during diagenesis in the absence of
359 post-depositional replacement of oxidizing agents (Tribovillard et al., 2006). The enrichment in
360 redox sensitive elements (Co/Al, Cr/Al, Cu/Al, U/Al, Th/Al, Mo_{EF}, Mo_{aut}, U_{EF} and U_{aut}) points
361 to depleted oxygen conditions during deposition of the Pre-Bahloul Member (base of the *W.*
362 *archaeocretacea* Biozone). U-based proxies (U_{EF}=8.08; Fig. 7) and increased TOC values point
363 to depleted oxygen conditions in the lower part of the water column.
364 The P/Ti ratio is a commonly used proxy for productivity (Latimer and Filippelli, 2001;
365 Robertson and Filippelli, 2008; Reolid et al., 2012a, b). Increased values are related to higher
366 phosphorous supply to the seafloor derived from biological processes, not from terrigenous
367 components (Latimer and Filippelli, 2001; Flores et al., 2005; Sen et al., 2008). At Oued
368 Bahloul, the increase in P/Ti values at the base of the *W. archaeocretacea* Biozone (Pre-
369 Bahloul Member) indicates an abrupt increase in productivity (Fig. 8). Mort et al. (2007)
370 suggested that the increase in P-accumulation rates coinciding with the OAE2 may be related to
371 an overall increase in surface-water productivity. At Oued Bahloul, high P/Ti values coincide
372 with high U/Al and U_{EF} values (Figs. 7 and 8), and point to a productivity increase in the Pre-
373 Bahloul Member. The Sr/Al ratio, which has also been used as a palaeoproductivity proxy (Sun
374 et al., 2008; Reolid et al., 2012), shows a minor increase in the Pre-Bahloul Member (Fig. 8).

375 This interpretation is compatible with the decreased foraminiferal diversity (both in
376 planktic and benthic assemblages) and with the assemblage turnover at the base of the *W.*
377 *archaeocretacea* Biozone (Figs. 4–6). Among benthic assemblages, the percentage of
378 *Gavelinella* spp. and *Lenticulina* spp. significantly increases in the Pre-Bahloul Member, and
379 *Globorotalites* shows a minor peak (Fig. 6). *Lenticulina* is regarded as an opportunistic genus
380 that recolonizes the seafloor after redox fluctuations (Tyszka, 1994; Reolid et al., 2008; Reolid
381 et al., 2012a). *Gavelinella* spp. is a low-oxygen tolerant genus (Sliter, 1975; Gertsch et al.,
382 2010), and it occurs in shales with high organic matter levels (Holbourn et al., 2001).
383 *Globorotalites* has been observed to peak under stressful conditions at the seafloor after the
384 Cretaceous/Paleogene impact event, mostly related to changes in the type (rather than in the
385 amount) of food supply (Alegret, 2007; Alegret et al., 2012). This assemblage composition,
386 together with the disappearance of some taxa at the *R. cushmani/W. archaeocretacea* biozone
387 boundary, indicate dysoxic conditions and a high food flux to the seafloor. The disappearance
388 of *Dorothia*, *Gyroidinoides*, *Laevidentalina*, *Lingulogavelinella*, and *Pyrulinoides* may be
389 related to the dysoxic conditions in the sea-bottom. The boundary between the Pre-Bahloul
390 Member and the Bahloul Member is characterised by the disappearance or abrupt decrease in
391 relative abundance of *Lenticulina*, *Gavelinella* and *Globorotalites*, and by an abrupt increase in
392 low-oxygen tolerant forms such as epifaunal *Neobulimina* (Fig. 6).
393 The planktic foraminiferal turnover across the Pre-Bahloul Member includes the
394 disappearance of specialist, intermediate to deep-dweller species adapted to oligotrophic
395 environments (*Rotalipora monsalvensis*), along with the temporary disappearance of
396 mesotrophic, intermediate-dwellers (*Praeglobotruncana gibba*, *Dicarinella* spp.). A peak in the
397 relative abundance of the specialist intermediate-dweller *Thalmanninella brotzeni* is recorded at
398 the base of the Pre-Bahloul Member just before its disappearance (Fig. 5). The percentages of
399 the eutrophic, surface-dweller species *Hedbergella delrioensis* (and *Whiteinella aprica* to a
400 minor extent) increase towards the top of the Pre-Bahloul Member, coinciding with the peaks in
401 redox proxies (Figs. 7 and 8), the disappearance of deep-dweller species (*R. cuhsmani*), and the

402 temporary disappearance of surface- and intermediate-dwellers (*Globigerinelloides* spp.,
403 *Praeglobotruncana stephani*). These data suggest that the deeper and intermediate layers of the
404 water column were more severely affected than surface waters at the *R. cushmani-W.*
405 *archaeocretacea* biozone transition, as suggested by Coccioni and Luciani (2004). An increase
406 in surface palaeoproductivity is supported by the disappearance of the large keeled *Rotalipora*, a
407 specialist genus probably living at or below the thermocline in oligotrophic conditions
408 (Coccioni and Luciani, 2004; Table 3), and by the increase in relative abundance of small-sized
409 *Hedbergella* and *Heterohelix*, opportunistic taxa adapted to eutrophic conditions (e.g. Hart,
410 1999; Keller et al., 2001; Table 3). An increase in P content in sections from the Tethys and
411 North Atlantic has been interpreted as indicative of changes in continental input (and nutrient
412 influx) or upwelling intensification during the late Cenomanian (Mort et al., 2007). Monteiro et
413 al. (2012) suggested that a high P content could be sustained by increased chemical weathering
414 and P regeneration from anoxic sediments.

415 The increase in P/Ti and U/Al in the Pre-Bahloul Member has good stratigraphic
416 correlation with increased redox proxies (Co/Al, Cr/Al, Ni/Al, and Th/Al), and shows a short
417 delay with respect to the increase in TOC values (Figs. 7 and 8). The marine anoxia of the
418 OAE2 is thought to have been related to enhanced biological productivity (e.g. Monteiro et al.,
419 2012; Pogge von Strandmann et al., 2013). Uranium and organic matter in the sediment are
420 related, as uranium may form a complex with dissolved fulvic acid in hemipelagic sediments
421 (Nagao and Nakashima, 1992). In this sense, high values for U/Al, U_{EF} and U_{aut} are congruent
422 with the high values of P/Ti.

423 In open-ocean systems with suboxic bottom waters, U_{aut} enrichment is greater than that
424 of Mo_{aut} because U_{aut} accumulation begins at the Fe(II)-Fe(III) redox boundary (Zhou et al.,
425 2012), while Mo_{aut} accumulation becomes more important as waters become euxinic. Higher
426 values of U_{aut} recorded in the Pre-Bahloul Member are congruent with oxygen-depleted
427 conditions not only at the sea-bottom waters but also in the deeper layers of the water column,

where deep dwellers such as *Rotalipora* inhabited. The relative abundance of surface dwellers such as *Hedbergella delrioensis* increased in the Pre-Bahloul Member.

5.2. Bahloul s. str. *Member*

Two intervals with significant peaks in redox proxies are recorded within the Bahloul Member (Fig. 7). The first one is located in the middle part of this unit (sample OB-17), and the second one is located towards its top, at the *W. archaeocretacea*/H. *helvetica* Biozone boundary (Fig. 7). Some redox proxies, such as Th/Al, U_{EF} and U_{aut}, do not show any significant changes across this interval.

In the lower half of the Bahloul Member (previous to sample OB-17), the amount of dissolved oxygen in the sea-bottom waters is interpreted to have been even lower than in the underlying Pre-Bahloul Member, as inferred from the disappearance of several benthic foraminiferal taxa and from the very low-diversity assemblages (Figs. 2 and 6), which are dominated by low-oxygen tolerant forms such as *Neobulimina* (Gertsch et al., 2010), *Praebulimina*, *Coryphostoma* and *Tappanina* spp. (incl. *T. laciniosa*). The clear dominance of *Neobulimina* and *Praebulimina* immediately above the extinction interval suggests that they may have behaved as disaster species, as suggested by Peryt and Lamolda (1996). According to these authors, disaster taxa evolved during the late, most stressful phases of an extinction interval, and persisted during the survival and recovery intervals. Species of *Coryphostoma* have small, tapered tests with abundant pores, and are common in dysaerobic environments (e.g., Leutenegger and Hansen, 1979; Bernhard, 1986). *Coryphostoma* is a common genus in low-oxygen environments during the early Danian (Coccioni et al., 1993; Alegret, 2007), and *Tappanina laciniosa* is a biserial, infaunal species that has been reported from dysoxic facies in highly eutrophic environments (e.g. Eicher and Worstell, 1970; Gustafsson et al., 2003; Friedrich and Erbacher, 2006). Moreover, the dominance of infaunal taxa in the Bahloul

454 Member and in the Annaba Member supports the interpretation of low oxygen conditions at the
455 seafloor (Jorissen et al., 1995).

456 The decreased abundance of the surface-dweller *Hedbergella delrioensis* at the base of
457 the Bahloul Member (Fig. 5) points to oxygen-depleted eutrophic surface waters, while low-
458 oxygen conditions only affected deep and intermediate waters in the underlying Pre-Bahloul
459 Member. Only *Heterohelix reussi* —opportunistic taxon adapted to eutrophic conditions—
460 proliferates in the lower part of Baloul Member in a context of decreasing diversity of planktic
461 foraminiferal assemblages.

462 Relatively higher TOC values (mean 1.42 wt.%) and high $\delta^{13}C$ are recorded in the
463 Bahloul Member (Fig. 8), suggesting higher productivity than in the other units and high
464 accumulation of organic matter derived from surface primary productivity (Schlanger and
465 Jenkyns, 1976; Arthur et al., 1990; Ingall et al., 1993; Van Cappellen and Ingall, 1994; Mort et
466 al., 2007). TOC values have been used as an indirect palaeoproductivity proxy by various
467 authors (e.g., Calvert and Fontugne, 2001; Gupta and Kawahata, 2006; Plewa et al., 2006; Su et
468 al., 2008; Reolid et al., 2012a) when TOC is related to phytodetritus associated with
469 phytoplankton or dinoflagellate remains. Nevertheless, because high TOC values may result
470 from low bottom-water ventilation and oxygen depletion, they are not necessarily related to
471 high surface productivity. According to Tribovillard et al. (2006), the TOC is generally
472 proportional to surface-water productivity and constitutes a useful palaeoproductivity proxy in
473 spite of certain complications attributable to efficient organic recycling, export productivity,
474 delivery to the sediment-water interface and final burial. The maximum TOC values (2.82
475 wt.%) are recorded at the base of this unit (Fig. 8), coeval with high percentages of *Heterohelix*
476 *reussi*, *Heterohelix moremani* and *Hedbergella planispira* (Fig. 5), which are thought to be
477 indicative of eutrophic environments (Table 3). These results are compatible with the analyses
478 of organic matter carried out by Farrimond et al. (1990), who reported abundant algal-derived
479 biological markers across the Cenomanian-Turonian transition at Oued Bahloul, suggesting high
480 surface productivity. High TOC values are also correlated to high percentages of *Neobulimina*

481 and other buliminids (Fig. 6), which are considered to be indicators of high-food and/or low
482 oxygenation at the seafloor in the modern oceans (e.g., Fontanier et al., 2002; Gooday, 2003).
483 The dominance of buliminids is also compatible with the proposed conditions, given that high
484 proportions of buliminids indicate eutrophic conditions (Sprong et al., 2013). These results point
485 to a high export productivity and poor oxygenation at the sea-bottom waters during deposition
486 of the lower part of the Bahloul Member; and combined with the high TOC and $\delta^{13}C$ values
487 (Figs. 8 and 9), they suggest a major climatic and palaeoceanographic perturbation in a
488 transgressive context (e.g. Zagrarni et al., 2008). In addition, Caron et al. (1999) and Soua et al.
489 (2011) documented the proliferation of radiolarians (mainly Nassellarian) and diatoms at the
490 base of the *Whiteinella archaeocretacea* Biozone (from the uppermost Pre-Bahloul Member), in
491 coincidence with an increased abundance of *Heterohelix* during the deposition of dark laminated
492 limestones. These authors interpreted the proliferation of radiolarians as indicative of renewal of
493 nutrient-rich oceanic waters and increase in water depth.

494 An increase in Mo_{EF} and Mo_{aut}, and a minor increase in Cu/Al, Cr/Al and Ni/Al are
495 observed in bed OB-17 (Fig. 7). High Mo_{EF} and Mo_{aut} values require the presence of H_2S
496 (euxinic conditions) (Tribovillard et al., 2012; Zhou et al., 2012). The gradual increase in Mo_{EF}
497 and Mo_{aut} across the lower half of the studied section indicates a progressive decrease in oxygen
498 availability towards euxinic conditions. Other authors have reported euxinic conditions from the
499 OAE2 (e.g. Wang et al., 2001; Scopelliti et al., 2004). The progressive accentuation of oxygen-
500 depleted conditions from the Pre-Bahloul Member towards the lower half of the Bahloul
501 Member is compatible with the disappearance of benthic taxa that flourished at the beginning of
502 the suboxic conditions (e.g., *Lenticulina*, *Gavelinella*, *Globorotalites*), and with the proliferation
503 of the disaster genus *Neobulimina* (low oxygen tolerant form, Friedrich et al., 2009), which has
504 been documented from other sections during the Cenomanian–Turonian event (e.g. Gebhardt et
505 al., 2004). Finally, the interpretation of anoxia/euxinia is compatible with the lack of benthic
506 foraminifera and very low diversity of planktic assemblages in sample OB-17. The bed OB-17
507 represents a benthic barren level. Unfavorable conditions also affected the water column during

508 this interval, as inferred from the dramatic decrease in the percentage of the opportunistic
509 surface dweller *Hedbergella delrioensis* and the increase in opportunistic surface to
510 intermediate dwellers (*Heterohelix* spp.). The highest relative abundances of heterohelicids (*H.*
511 *reussi*) occur in OB-17 (Fig. 5), where maximum values of Mo_{EF} and Mo_{aut} are recorded (Fig.
512 7). *Heterohelix* has been interpreted as a low-oxygen tolerant genus that bloomed in stratified
513 open marine settings with a well-developed oxygen minimum zone (e.g. Leckie et al., 1998;
514 Premoli Silva and Sliter, 1999; Keller et al., 2001; Keller and Pardo, 2004).
515 Redox proxies indicate the return to normal oxygen conditions across the upper half of
516 the Bahloul Member, but the palaeoenvironmental perturbation induced slow recovery of the
517 foraminiferal assemblages, as reflected by the dominance of the opportunistic *Heterohelix* and
518 *Whiteinella* in intermediate and surface waters, respectively. Diversity of benthic assemblages
519 slightly increases through this interval, and assemblages are dominated by buliminids
520 (*Neobulimina* and *Praebulimina*), with higher percentages of *Gavelinella rochardensis,*
521 *Laevidentalina* and *T. laciniosa* towards the upper part of the Bahloul Formation. The species *T.*
522 *laciniosa* and the genera *Gavelinella*, *Neobulimina* and *Praebulimina* have been reported from
523 dysoxic facies in highly eutrophic environments and high organic-matter fluxes (e.g. Eicher and
524 Worstell, 1970; Coccioni et al., 1993; Gustafsson et al., 2003; Gebhardt et al., 2004; Friedrich
525 and Erbacher, 2006; Friedrich et al., 2009). This assemblage suggests that the repopulation
526 phase at the seafloor occurred in the upper half of the Bahloul Formation. Among planktic
527 foraminifera, the opportunistic surface dweller *Whiteinella* proliferated in this interval, together
528 with the intermediate dweller *H. reussi*, as previously reported from the Tethys area (Coccioni
529 and Luciani, 2004). Non-opportunist forms including *Praeglobotruncana* and *Dicarinella* are
530 recorded in the upper part of the *W. archaeocretacea* Biozone, whereas deep dweller specialists
531 as *Rotalipora* are definitively extinct and there are no genera occupying this ecologic niche.
532 A positive peak in redox proxies (Mo_{EF}, Cu/Al, Co/Al, Cr/Al, Ni/Al ratios) and a minor
533 increase in some palaeoproductivity proxies have been recorded at the *W. archaeocretacea*/*H.*
534 *helvetica* biozone boundary (sample OB-33), coinciding with an increase in the percentage of

535 buliminids and *Guembelitria cenomana*. *Guembelitria* is interpreted as an opportunist surface
536 dweller adapted to poorly oxygenated, eutrophic waters (Table 3) or to variable salinity and
537 nutrient levels (Keller and Pardo, 2004). The obtained data indicate high productivity and low-
538 oxygen conditions both in surface waters and at the seafloor towards the top of the *W.*
539 *archaeocretacea* Biozone. According to Soua et al. (2011), the composition of radiolarian
540 assemblages also experiments a turnover related to low-oxygen conditions with a drastic
541 decrease of nassellarians and an abundance and diversification of spumellarians.
542
543 *5.3. Base of the Kef Formation*
544
545 A progressive increase in the diversity of planktic assemblages, together with the co-
546 occurrence of surface and intermediate-to-deep dwellers indicates partial recovery of the
547 assemblages at the beginning of the *H. helvetica* Biozone. The most common taxa (*Whiteinella,*
548 *Heterohelix, Hedbergella*) are indicative of eutrophic, oxygenated to poorly oxygenated surface
549 and intermediate waters. Deep dwellers such as the intermediate to specialist
550 *Helvetoglobotruncana* (Table 3) make only a minor contribution to the assemblages. Just after
551 the last suboxic pulse of the top of Bahloul Member (level OB-33), *Whiteinella* proliferates
552 again in the assemblage as a rapid response to improved conditions.
553 In benthic microhabitats, the beginning of the *H. helvetica* Biozone is marked by an
554 increase in relative abundance of *Gyroidinoides*, *Lenticulina* and *Planularia*, and a decrease in
555 *Tappanina* and *Gavelinella.* Diversity of the benthic assemblages remains low, and the
556 dominance of buliminids (*Praebulimina* and *Neobulimina*) indicates a high food supply or low-
557 oxygen conditions at the seafloor (Jorissen et al., 1995; Widmark and Speijer, 1997; Fontanier
558 et al., 2002).
559
560 **6. Climatic and palaeoceanographic changes across the Cenomanian–Turonian boundary**
561

562 Analyses of $\delta^{18}O$ in bulk rock show a ~ 1.5 ‰ decrease from the base of the section
563 towards the Bahoul Member, followed by a gradual recovery above this unit (Fig. 9). Assuming
564 these results have not been strongly altered by diagenesis, we infer significantly warmer (~ 6ºC)
565 temperatures during deposition of the organic rich facies of the Bahoul Member (*W.*
566 *archaeocretacea* Biozone), coeval with the disappearance of specialist planktic foraminifera
567 (e.g. *Rotalipora*) and with the proliferation of opportunistic, eutrophic forms such as
568 *Heterohelix* and *Hedbergella*. These results suggest a narrow link between the development of
569 the anoxic event and eutrophic conditions with changes in the ocean-atmosphere system. Some
570 authors have identified a short term cooling during the OAE2 (e.g. Jarvis et al., 2011; Gavrilov
571 et al., 2013; Zheng et al., 2013), which we were not able to recognize in our record from Oued
572 Bahloul at the present resolution.
573 In the transgressive context of the Cenomanian–Turonian boundary (e.g. Zagrarni et al.,
574 2008), the enhanced fertility resulting in high primary productivity and eutrophication was
575 favored by nutrient inputs by leaching from flooded shelves (Erbacher et al., 2001) or enhanced
576 continental supply of nutrients (Föllmi, 1995; Handoh and Lenton, 2003). According to Wagner
577 et al. (2007), the warm humid climate contributes to an intensified hydrological cycle and
578 enhanced export of nutrient-rich weathered material from land to the ocean, as also suggested
579 for the Paleocene-Eocene Thermal Maximum (see refs. in Arreguín-Rodríguez et al., 2014). For
580 the end of Cenomanian, another hypothesis was developed by Caron et al. (1999): the
581 alternation of climatic fluctuations, with evaporation/precipitation in low latitude areas and the
582 formation of dense, hypersaline sea waters.
583 Calcareous nannofossil turnover has been interpreted in terms of enhanced fertility and
584 increased temperatures, pointing to an eutrophication event (Erba, 2004; Hardas and Mutterlose,
585 2007). P-cycling models for Cretaceous Anoxic Events, however, indicate that enhanced
586 primary productivity is not enough for producing anoxic conditions in the bottom waters if
587 water circulation exists (Tsandev and Slomp, 2009). According to these authors, the global
588 ocean has to be sufficiently stagnant (low mixing) to allow the system to achieve oxygen

589 depletion in the deep sea. In general, the thermohaline circulation during the Cretaceous is
590 believed to have been slower due to reduced thermal gradients between the tropics and poles
591 (e.g. Shlanger and Jenkyns, 1976; Fischer and Arthur, 1977), and the wider extension of
592 continental shelves (e.g. Bjerrum et al., 2006). In this context, increased P supply from flooded
593 shelves and weathered continental areas may have triggered enhanced primary production and
594 anoxia in a stagnant ocean. In the Oued Bahloul section, a significant increase in P has been
595 observed in the Pre-Bahloul Member coeval with high dominance of *Hedbergella* and the
596 extinction of *Rotalipora*. The progressive decrease in oxygenation of bottom- and deep-waters
597 towards anoxic conditions in the Bahloul Member (metre 17, OB-17) represents the most
598 stressing conditions for the foraminiferal assemblages, with the disappearance of benthic
599 foraminifera, the expansion of the oxygen minimum zone coincident with maximum values of
600 *Heterohelix,* and probably euxinic conditions in the low water column as indicated by increased
601 Mo_{EF} and $Mo_{aut.}$
602
603 **7. Conclusions**
604
605 The integrated analysis of planktic and benthic foraminiferal assemblages, geochemical
606 proxies, TOC and $\delta^{13}C$ and $\delta^{18}O$ from the classic locality of the Oued Bahloul section allowed
607 us to interpret: (a) the redox and palaeoproductivity fluctuations related to the C/T boundary,
608 and (b) the ecostratigraphic changes of foraminiferal associations across the OAE2.
609 Significant changes were recorded across the *R. cushmani*/*W. archaeocretacea*
610 boundary, and planktic and benthic foraminiferal diversity decreased. The disappearance of the
611 planktic genera *Rotalipora*, *Praeglobotruncana*, *Globigerinelloides* and *Thalmanninella*, and
612 the occurrence of the opportunist genus *Hedbergella*, together with the proliferation of
613 buliminids and the increase in palaeoproductivity proxies (P/Ti, U/Al, Sr/Al), indicate eutrophic
614 conditions both in the water column and at the seafloor. The abundance of low-oxygen tolerant
615 genera of benthic foraminifera at the base of *W. archaeocretacea* Biozone is compatible with

616 the enrichment in redox proxies indicating dysoxic conditions in sediment pore water. Deep
617 waters were also oxygen-depleted, as deduced from higher values of U_{aut} than Mo_{aut}, favouring
618 the disappearance of *Rotalipora* and *Globigerinelloides* and the proliferation of surface-dweller
619 *Hedbergella*. The maximum TOC values registered in the lower part of the *W. archaeocretacea*
620 Biozone indicate an abrupt increase in organic matter coeval with an increase in
621 palaeoproductivity and redox proxies.

622 The persistence of the poorly oxygenated conditions in the *W. archaeocretacea* Biozone
623 probably produced euxinic conditions, as indicated by high Mo_{EF} and Mo_{aut} values, minimum
624 diversity and the local disappearance of benthic forms. The decrease in abundance of
625 opportunist surface dwellers (*Hedbergella*) and the increase in opportunist intermediate dwellers
626 (heterohelicids), together with maximum values of Mo_{EF} and Mo_{aut}, indicate stressed conditions
627 and stratified open marine settings with a well-developed oxygen minimum zone.

628 The redox proxies indicate a return to normal oxygen conditions in the upper part of the
629 *W. archaeocretacea* Biozone, with a slow recovery of foraminiferal assemblages. The genus
630 *Whiteinella*, characteristic of mesotrophic environments, becomes more abundant upward in the
631 section. The subsequent colonization of the bottom after the anoxic event was produced by
632 *Praebulimina* (disaster genus), *Gavelinella*, *Neobulimina* and *Tappanina*. These genera are
633 low-oxygen tolerant and related to high organic matter fluxes, thus representing the
634 repopulation episode of the bottom after the benthic barren interval.

635 The *W. archaeocretacea*/*H. helvetica* biozone boundary is characterized by increasing
636 values of redox proxies, coeval with a new peak of *Praebulimina*, a decrease in *Whiteinella* and
637 the record of opportunist *Guembelitria*.

638 The beginning of the *H. helvetica* Biozone indicates a partial recovery of the planktic
639 foraminiferal assemblage due to a persistent dominance of opportunists (*Whiteinella* and
640 *Hedbergella* in surface waters, and *Heterohelix* in intermediate waters). In benthic
641 microhabitats, the beginning of the *H. helvetica* Biozone is marked by an increase in relative
642 abundance of *Neobulimina*, *Lenticulina*, and *Gyroidinoides,* and a decrease in *Tappanina*.

643 Temperature changes and palaeoceanographic reorganization have been inferred across
644 the OAE2. This entailed a low mixing of surface and deep waters (poor ocean ventilation) and
645 enhanced primary productivity related to global warming, increasing continental weathering and
646 nutrient input to the ocean. The expansion of the oxygen minimum zone and the eutrophication
647 led to a reduced diversity of foraminifera and the planktic foraminiferal shift, showing a
648 dominance of genera with low-oxygen tolerance typical of high mesotrophic to eutrophic
649 conditions.
650
651 **Acknowledgements**
652
653 We thank Dalila Zaghbib-Turki (Université de Tunis El Manar) and Mohamed Soua
654 (Entreprise Tunisienne d'Activités Pétrolières), who helped us sample the Oued Bahloul
655 section. This research was supported by Projects RYC-2009-04316 (Ramón y Cajal Program,
656 Ministerio de Ciencia e Innovación + FSE), Project CGL2012-33281 (Secretaría de Estado de
657 I+D+I, Spain), P11-RNM-7408 (Junta de Andalucía), and Projects CGL2011-23077 and
658 CGL2011-22912 of the Spanish Ministry of Science and Technology (FEDER funds) and the
659 consolidated group E05 funded by the Government of Aragon. Sánchez-Quiñónez, C.A. thanks
660 the Fundación Carolina (Spain) for a grant for supporting his research stay at the Universidad de
661 Zaragoza. We thank the editor Finn Surlyk and the reviewers Michèle Caron (Universität
662 Freiburg) and an anonymous reviewer for comments. The authors thank Jean Louise Sanders for
663 improving English language.
664
665
666 **References**
667
668 Accarie, H., Emmanuel, L., Robaszynski, F., Baudin, F., Amédro, F., Caron, M., Deconinck,
669 J.F., 1996. La géochimie isotopique du carbone ($\delta^{13}C$) comme outil stratigraphique.

Aplication à la limite Cénomanien/Turonien en Tunisie central. Comptes Rendus Academie des Sciences, Paris 322, 579–586.

Accarie, H., Robaszynski, F., Amédro, F., Caron, M., Zagrarni, M.F., 2000. Stratigraphie événementielle au passage Cénomanien-Turonien dans le secteur occidental de la plate-forme de la Tunisie centrale (Formation Bahloul, région de Kalaat Senan). Annales des Mines et de la Geologie, Tunisie 40, 63–80.

Alegret, L., 2007. Recovery of the deep-sea floor after the Cretaceous/Paleogene boundary event: the benthic foraminiferal record in the Basque-Cantabrian basin and in South-eastern Spain. Palaeogeography, Palaeoclimatology, Palaeoecology 255, 181–194.

Alegret, L., Thomas, E., Lohmann, K.C., 2012. End-Cretaceous marine mass extinction not caused by productivity collapse. Proceedings of the National Academy of Sciences 109, 728–732

Amédro, F., Accarie, H., Robaszynski, F., 2005. Position de la limite Cénomanien-Turonien dans le Formation Bahloul de Tunisie centrale : apports intégrés des ammonites et des isotopes du carbone ($\delta^{13}C$). Eclogae Geologicae Helvetiae 98, 151–167.

Arreguín-Rodríguez, G.J., Alegret, L., Sepúlveda, J., Newman, S., Summons, R. E. 2014. Enhanced terrestrial input supporting the *Glomospira* acme across the Paleocene-Eocene boundary in Southern Spain. Micropaleontology 60, 43–51.

Arthur, M.A., Jenkyns, H.C., Brumsack, H.J., Schlanger, S.O., 1990. Stratigraphy, geochemistry, and paleoceanography of organic carbon-rich Cretaceous sequences. In: Ginsburg, R.N., Beaudoin, B., (eds.), Cretaceous Ressources, Events and Rhythms: Background and Plans for Research, NATO ASI series, pp. 75–119.

Bernhard, J.M., 1986. Characteristic assemblages and morphologies of benthic foraminifera from anoxic, organic rich deposits: Jurassic trough Holocene. Journal of Foraminiferal Research 16, 207–215.

695 Bjerrum, C.J., Bendtsen, J., Legarth, J.J.F., 2006. Modeling organic carbon burial during sea
696 level rise with reference to the Cretaceous. Geochemistry, Geophysics, Geosystems 7,
697 Q05008.
698 Bornemann, A., Norris, R.D., Friedrich, O., Beckmann, B., Schouten, R., Sinninghe-Damste, J.,
699 Vogel, J., Hofmann, P., Wagner, T., 2008. Isotopic evidence for glaciation during the
700 Cretaceous super-greenhouse. Science 319, 951–954.
701 Burollet, P.F., 1956. Contribution à l'étude stratigraphique de la Tunisie Centrale. Annales des
702 Mines et de la Géologie, Tunisie 18, 1–345.
703 Burollet, P.F., Busson, G., 1983. Plate-forme Saharienne et Mésogée au cours du Crétacé. Notes
704 et Memoires Total-CFP 18, 17–26.
705 Calvert, S.E., 1990, Geochemistry and origin of the Holocene sapropel in the Black Sea. In
706 Ittekkot, V., Kempe, S., Michaelis, W., and Spitzy, A. (eds.), Facets of Modern
707 Biogeochemistry, Springer, Berlin, pp. 326–352.
708 Calvert, S.E., Fontugne, M.R., 2001. On the late Pleistocene-Holocene sapropel record of
709 climatic and oceanographic variability in the eastern Mediterranean. Paleoceanography 16,
710 78–94.
711 Calvert, S.E., Pedersen, T.F., 1993. Geochemistry of recent oxic and anoxic marine sediments:
712 Implications for the geological record. Marine Geology 113, 67–88.
713 Caron, M., 1983. La spéciation chez les Foraminifères planctiques: une réponse adaptée aux
714 contraintes de l´environnement. Zitteliana 10, 671–676.
715 Caron, M., Homewood, P., 1983. Evolution of early planktic foraminifers. Marine
716 Micropaleontology 7, 453–462.
717 Caron, M., Dall'Agnolo, S., Accarie, H., Barrera, E., Kauffman, E.G., Amédro, F.,
718 Robaszynski, F., 2006. High-resolution stratigraphy of the Cenomanian_Turonian
719 boundary interval at Pueblo (USA) and wadi Bahloul (Tunisia): stable isotope and bio-
720 events correlation. Geobios 39, 171–200.

721 Caron, M., Robaszynski, F., Amédro, F., Baudin, F., Deconinck, J.F., Hochli, P., Von Salis-
722 Perch Nielsen, K., Tribovillard, N., 1999. Estimation de la durée de l'événement anoxique
723 global au passage Cénomanien-Turonien. Approche cyclostratigraphique dans la Formation
724 Bahloul en Tunisie centrale. Bulletin de la Société Géologique de France 170, 145–160.
725 Coccioni, R., Fabbrucci, L., Galeotti, S., 1993. Terminal Cretaceous deep-water benthic
726 foraminiferal decimation, survivorship and recovery at Caravaca (SE Spain). Paleopelagos
727 3, 3–24.
728 Coccioni, R., Luciani, V., 2004. Planktonic foraminifera and environmental changes across the
729 Bonarelli Event (OAE2, Latest Cenomanian) in its type area: a high-resolution study from
730 the Tethyan reference Bottaccione section (Gubbio, Central Italy). Journal of Foraminiferal
731 Research 34, 109–129.
732 Corliss, B.H., 1985. Microhabitat of benthic foraminifera with deep sea sediments. Nature 314,
733 435–438.
734 Corliss, B.H., 1991. Morphology and microhabitat preferences of benthic foraminifera from the
735 northwest Atlantic Ocean. Marine Micropaleontology 17, 195–236.
736 Corliss, B.H., Chen, C., 1988. Morphotype patterns of Norwegian deep sea benthic foraminifera
737 and ecological implications. Geology 16, 716–719.
738 Eicher, D.L., Worstell, P., 1970. Cenomanian and Turonian foraminfiera from the Great Plains,
739 United States. Micropaleontology 16, 269–324.
740 Erba, E., 2004. Calcareous nannofossils and Mesozoic oceanic anoxic events. Marine
741 Micropaleontology 52, 85–106.
742 Erba, E., Bottini, C., Faucher, G., 2013. Cretaceous large igneous provinces: The effects of
743 submarine volcanism on calcareous nannoplankton. Mineralogical Magazine 77, p. 1044.
744 Erbacher, J., Huber, B.T., Norris, R.D., Markey, M., 2001. Increased thermohaline stratification
745 as a possible cause for an ocean anoxic event in the Cretaceous period. Nature 409, 325–
746 327.

747 Farrimond, P., Eglinton, G., Brassell, S.C., 1990. The Cenomanian/Turonian anoxic event in
748 Europe: an organic geochemical study. Marine and Petroleum Geology 7, 75–89.
749 Fischer, A.G., Arthur, M.A., 1977. Secular variations in the pelagic realm. In: Cook, H.E. (ed.),
750 Deep-water carbonate environments. SEPM Sp. Pub. 25, 19–50.
751 Flores, J.A., Sierro, F.J., Filippelli, G.M., Barcena, M.A., Pérez-Folgado, M., Vázquez, A.,
752 Utrilla, R., 2005. Surface water dynamics and phytoplankton communities during
753 deposition of cyclic late Messinian sapropel sequences in the western Mediterranean.
754 Marine Micropaleontology 56, 50–79.
755 Föllmi, K.B., 1995. 160 m.y. record of marine sedimentary phosphorous burial: coupling of
756 climate and continental weathering under greenhouse and icehouse conditions. Geology 23,
757 859–862.
758 Fontanier, C., Jorissen, F.J., Licari, L., Alexandre, A., Anschutz, P., Carbonel, P., 2002. Live
759 benthic foraminiferal faunas from the Bay of Biscay: faunal density, composition and
760 microhabitats. Deep-Sea Research. Part 1. Oceanographic Research Papers 49, 751–785.
761 Friedrich, O., Erbacher, J., 2006. Benthic foraminiferal assemblages from Demerara Rise (ODP
762 Leg 207, western Tropical Atlantic): possible evidence for a progressive opening of the
763 Equatorial Atlantic Gateway. Cretaceous Research 27, 377–397.
764 Friedrich, O., Erbacher, J., Wilson, P.A., Moriya, K., Mutterlose, J., 2009. Paleoenvironmental
765 changes across the Mid Cenomanian Event in the tropical Atlantic Ocean (Demerara Rise,
766 ODP Leg 207) inferred from benthic foraminiferal assemblages. Marine Micropaleontology
767 71, 28–40.
768 Gallego-Torres, D., Martínez-Ruiz, F., Paytan, A., Jiménez-Espejo, F.J., Ortega-Huertas, M.,
769 2007. Pliocene–Holocene evolution of depositional conditions in the eastern Mediterranean:
770 Role of anoxia vs. productivity at 632 time of sapropel deposition. Palaeogeography,
771 Palaeoclimatology, Palaeoecology 246, 424–439.

772 Gavrilov, Y.O., Shcherbinina, E.A., Golovanova, O.V., Pokrovskii, B.G., 2013. The Late
773 Cenomanian paleoecological event (OAE 2) in the eastern Caucasus basin of Northern Peri-
774 Tethys. Lithology and Mineral Resources 48, 457–488.
775 Gebhardt, H., Kuhnt, W., Holbourn, A., 2004. Foraminiferal response to sea level change,
776 organic flux and oxygen deficiency in the Cenomanian of the Tarfaya Basin, southern
777 Morocco. Marine Micropaleontology 53, 133–157.
778 Gebhardt, H., Friederich, O., Schenk, B., Fox, L., Hart, M., Wagreich, M., 2010.
779 Paleoceanographic changes at the northern Tethyan margin during the Cenomanian-
780 Turonian Oceanic Anoxic Event (OAE2). Marine Micropaleontology 77, 25–45.
781 Gertsch, B., Keller, G., Adatte, T., Berner, Z., Kassab, A.S., Tantawy, A.A.A., El-Sabbagh,
782 A.M., Stueben, D., 2010. Cenomanian-Turonian transition in a shallow water sequence of
783 the Sinai, Egypt. International Journal of Earth Sciences 99, 165–182.
784 Gooday, A., 2003. Benthic foraminifera (Protista) as tools in deep-water palaeoceanography:
785 environmental influences on faunal characteristics. Advances in Biology 46, 1–90
786 Gupta, L.P., Kawahata, H., 2006. Downcore diagenetic changes in organic matter and
787 implications for paleoproductivity estimates. Global and Planetary Change 53, 122–136.
788 Gustafsson, M., Holbourn, A., Kuhnt, W., 2003. Changes in Northeast Atlantic temperature and
789 carbon flux during the Cenomanian/Turonian paleoceanographic event: the Goban Spur
790 stable isotope record. Palaeogeography, Palaeoclimatology, Palaeoecology 201, 51–66.
791 Hallam, A., 1992. Phanerozoic sea level changes. Columbia Press, New York, 266 pp.
792 Handoh, I.C., Lenton, T.M., 2003. Periodic mid-Cretaceous oceanic anoxic events linked by
793 oscillations of the phosphorous and oxygen biogeochemical cycles. Global Biogeochemical
794 Cycles 17, doi:10.1029/2003GB002039
795 Hardas, P., Mutterlose, M.J., 2007. Calcareous nannofossil assemblages of Oceanic Anoxic
796 Event 2 in the equatorial Atlantic: Evidence of an eutrophication event. Marine
797 Micropaleontology 66, 52–69.

798 Hardenbol, J., Thierry, J., Farley, M.B., Jacquin, T., de Graciansky, P.C., Vail, P.R., 1998.
799 Mesozoic and Cenozoic sequence chronostratigraphic framework of European Basins. In:
800 Graciansky, P.C., Hardenbol, J., Jacquin, T., Vail, P.R. (eds.), Mesozoic and Cenozoic
801 Sequence Stratigraphy of European Basins. SEPM Sp. Publ. 60, 3–13.
802 Hart, M.B., 1996. Recovery of the food chain after the late Cenomanian extinction event. In:
803 Hart, M.B. (ed.), Biotic recovery from Mass Extinction Events. Geological Society of
804 London Sp. Publ. 102, 265–277.
805 Hart, M.B., 1999. The evolution and diversity of Cretaceous planktonic foraminiferida. Geobios
806 32, 247–255.
807 Hart, M.B., Bailey, H.W., 1979. The distribution of planktonic Foraminiferida in the Mid-
808 Cretaceous of NW Europe. In: Wiedmann, J. (ed.), Aspekte der Kreide Europas.
809 International Union of Geological Sciences, Series A, 6, 527–542.
810 Hemleben, C., Spindler, M., Anderson, O.R., 1989. Modern planktonic foraminifera. Springer-
811 Verlag, Berlin, 363 pp.
812 Holbourn, A., Kuhnt, W., 2002. Cenomanian-Turonian palaeoceanographic change on the
813 Kerguelen Plateau a comparison with Northern Hemisphere records. Cretaceous Research
814 23, 333–349.
815 Holbourn, A., Kuhnt, W., Erbacher, J., 2001. Benthic foraminifers from lower Albian black
816 shales (Site 1049, ODP leg 171): evidence for a non ‘uniformitarian’ record. Journal of
817 Foraminiferal Research 31, 60–74.
818 Huber, B.T., Norris, R.D., McLeod, K.G., 2002. Deep-sea paleotemperature record of extreme
819 warmth during the Cretaceous. Geology 30, 123–126.
820 Ingall, E.D., Bustin, R.M., Van Cappellen, P., 1993. Influence of water column anoxia on the
821 burial and preservation of carbon and phosphorus in marine shales. Geochimica et
822 Cosmochimica Acta 57, 303–316.

823 Jarvis, I., Lignum, J.S., Groecke, D.R., Jenkyns, H.C., Pearce, M.A., 2011. Black shale
824 deposition, atmospheric CO2 drawdown, and cooling during the Cenomanian-Turonian
825 Oceanic Anoxic Event. Paleoceanography 26, PA3201.
826 Jones, R.W., Charnock, M.A., 1985. "Morphogroups" of agglutinating foraminifera. Their life
827 position and feeding habits and potential applicability in (paleo)ecological studies. Revue
828 Paléobiologie 4, 311–320.
829 Jones, B.A., Manning, D.A.C., 1994. Comparison of geochemical indices used for the
830 interpretation of paleoredox conditions in ancient mudstones. Chemical Geology 111, 111–
831 129.
832 Jorissen, F.J., De Stigter, H.C., Widmark, J.G.V., 1995. A conceptual model explaining benthic
833 foraminiferal habitats. Marine Micropaleontology 26, 3–15.
834 Kaiho, K., 1994. Planktonic and benthic foraminiferal extinction events during the last 100 m.y.
835 Palaeogeography, Palaeoclimatology, Palaeoecology 111, 45–71.
836 Kaiho, K., 1999. Evolution in the test size of deep-sea benthic foraminifera during the past 120
837 m.y. Marine Micropaleontology 37, 53–65.
838 Keller, G., Han, Q., Adatte, T., Burns, S.J., 2001. Paleoenvironment of the Cenomanian-
839 Turonian transition at Eastbourne, England. Cretaceous Research 22, 391–322.
840 Keller, G., Pardo, A., 2004. Age and environment of the Cenomanian-Turonian global
841 stratotype section and point at Pueblo, Colorado. Marine Micropaleontology 51, 95–128.
842 Klein, C., Mutterlose, J., 2001. Benthic foraminifera: indicators for a long-term improvement of
843 living conditions in the late Valanginian of the NW German Basin. Journal of
844 Micropalaeontology 20, 81–95.
845 Kuroda, J., Ogawa, N.O., Tanimizu, M., Coffin, M.T., Tokuyama, H., Kitazato, H., Ohkouchi,
846 N., 2007. Contemporaneous massive subaerial volcanism and late Cretaceous Oceanic
847 Anoxic Event 2. Earth Planetary Science Letters 256, 211–223.

848 Kuypers, M.M.M., Pancost, R.D., Nijenhuis, I.A., Sinninghe-Damste, J.S., 2002. Enhanced
849 productivity led to increased organic carbon burial in the euxinic North Atlantic Basin
850 during the late Cenomanian oceanic anoxic event. Paleoceanography 17, 1051.
851 Latimer, J.C., Filippelli, G.M., 2001. Terrigenous input and paleoproductivity in the Southern
852 Ocean. Paleoceanography 16, 627–643.
853 Leckie, R., Yuretich, R.F., West, O.L.O., Finkelstein, D., Schmidt, M., 1998. Paleoceanography
854 of the southwestern Western Interior Sea during the time of the Cenomanian-Turonian
855 boundary (Late Cretaceous). In: Dean, W., Arthur, M.A. (eds.) Stratigraphy and
856 Paleoenvironments of the Cretaceous Western Interior Seaway, USA. Society for
857 Sedimentary Geology, Concepts in Sedimentology and Paleontology 6, Tulsa, 101–126.
858 Leutenegger, S., Hansen, H.J., 1979. Ultrastructural and radiotracer studies of pore function in
859 foraminifera. Marine Biology 54, 11–16.
860 Monteiro, F.M., Pancost, R.D., Ridwell, A., Donnadieu, Y., 2012. Nutrients as the dominant
861 control on the spread of anoxia and euxinia across the Cenomanian-Turonian oceanic
862 anoxic event (OAE2): model-data comparison. Paleoceanography 27, PA4209.
863 Mort, M., Adatte, T., Föllmi, K.B., Keller, G., Steinmann, P., Matera, V., Berner, Z., Stüben,
864 D., 2007. Phosphorous and the roles of productivity and nutrient recycling during oceanic
865 event 2. Geology 35, 483–486.
866 Murray, J.W., 1991. Ecology and palaeoecology of benthic foraminifera. Longman, Harlow,
867 397 pp.
868 Nagao, S., Nakashima, S., 1992. Possible Complexation of Uranium with Dissolved Humic
869 Substances in Pore Water of Marine-Sediments. Science of the Total Environment 118,
870 439–447.
871 Nagy, J., 1992. Environmental significance of foraminiferal morphogroups in Jurassic North
872 Sea deltas. Palaeogeography, Palaeoclimatology, Palaeoecology 95, 111–134.

873 Nederbragt, A.J., Fiorentino, A., 1999. Stratigraphy and paleoceanography of the Cenomanian-
874 Turonian Boundary Event in Oued Mellegue, north-western Tunisia. Cretaceous Research
875 20, 47–62.
876 Negra, M.H., Zagrarni, M.F., Hanini, A., Strasser, A., 2011. The filament event near the
877 Cenomanian-Turonian boundary in Tunisia: filament origin and environmental
878 signification. Bulletin Société Géologique France 182, 507–519.
879 Norris, R.D., Bice, K.L., Magno E.A., Wilson, P.A., 2002. Jiggling the tropical thermostat in
880 the Cretaceous hothouse. Geology 30, 299–302.
881 Peryt, D., 2004. Benthic foraminiferal response to the Cenomanian-Turonian and Cretaceous-
882 Paleogene boundary events. Przegląd Geologiczny 52, 827–832.
883 Peryt, D., Lamolda, M., 1996. Benthonic foraminiferal mass extinction and survival
884 assemblages from the Cenomanian-Turonian Boundary Event in the Menoyo section,
885 northern Spain. Geological Society, London, Special Publications 102, 245–258.
886 Petrizzo, M.R., 2002. Palaeoceanographic and palaeoclimatic inferences from Late Cretaceous
887 planktonic foraminiferal assemblages from the Exmouth Plateau (ODP Sites 762 and 763,
888 eastern Indian Ocean). Marine Microplaeontology 45, 117–150.
889 Plewa, K., Meggers, H., Kasten, S., 2006. Barium in sediments off northwest Africa: A tracer
890 for palaeoproductivity or meltwater events? Paleoceanography 21, PA2015.
891 Pogge von Strandmann, P.A.E., Jenkyns, H.C., Woodfine, R.G., 2013. Lithium isotope evidence
892 for enhanced weathering during Oceanic Anoxic Event 2. Nature Geoscience 6, 668–672.
893 Powell, W.G., Johston, P.A., Collom, C.J., 2003. Geochemical evidence for oxygenated bottom
894 waters during deposition of fossiliferous strata of the Burgess Shale Formation.
895 Palaeogeography, Palaeoclimatology, Palaeoecology 201, 249–268.
896 Premoli Silva, I., Sliter, W.V., 1999. Cretaceous Paleoceanography: evidence from planktonic
897 foraminiferal evolution. In: Barrera, E., Johnson C.C. (eds.), Evolution of the Cretaceous
898 Ocean-Climate System. Geological Society America Sp Paper 332, 301–328.

899 Reolid, M., Martínez-Ruiz, F., 2012. Comparison of benthic foraminifera and geochemical
900 proxies in shelf deposits from the Upper Jurassic of the Prebetic (southern Spain). Journal of
901 Iberian Geology 38, 449–465.
902 Reolid, M., Rodríguez-Tovar, F.J., Nagy, J., Olóriz, F., 2008. Benthic foraminiferal
903 morphogroups of mid to outer shelf environments of the Late Jurassic (Prebetic Zone,
904 Southern Spain): Characterisation of biofacies and environmental significance.
905 Palaeogeography, Palaeoclimatology, Palaeoecology 261, 280–299.
906 Reolid, M., Rodríguez-Tovar, F.J., Marok, A., Sebane, A., 2012a. The Toarcian Oceanic
907 Anoxic Event in the Western Saharan Atlas, Algeria (North African Paleomargin): role of
908 anoxia and productivity. Geological Society of America Bulletin 124, 1646–1664.
909 Reolid, M., Rodríguez-Tovar, F.J., Nagy, J., 2012b. Ecological replacement of Valanginian
910 agglutinated foraminifera during a maximum flooding event in the Boreal realm
911 (Spitsbergen). Cretaceous Research 33, 196–204.
912 Robaszynski, F., Caron, M., Amédro, F., Dupuis, C., Hardenbol, J., González-Donoso, J.M.,
913 Linares, D., Gartner, S., 1993. Le Cénomanien de la región de Kalaat Senan (Tunisie
914 Centrale): Litho-biostratigraphie et interprétation séquentielle. Revue de Paléobiologie 12,
915 351–505.
916 Robaszynski, F., Caron, M., Dupuis, C., Amédro, F., González-Donoso, J.M., Linares, D.,
917 Hardenbol, J., Gartner, S., Calandra, F., Deloffre, 1990. A tentative integrated stratigraphy
918 in the Turonian of central Tunisia: Formations, zones and sequential stratigraphy in the
919 Kalaat Senan area. Bull. Centre Recherche Exploration-Production Elf-Aquitaine 14, 213–
920 384.
921 Robaszynski, F., Zargrani, M.F., Caron, M., Amédro, F., 2010. The global bio-events at the
922 Cenomanian-Turonian transition in the reduced Bahloul Formation of Bou Ghanem
923 (central Tunisia). Cretaceous Research 31, 1-15.

924 Robertson, A.K., Filippelli, G.M., 2008. Paleoproductivity variations in the eastern equatorial
925 Pacific over glacial timescales: American Geophysical Union Fall Meeting 2008, Abstract
926 PP33C-1576.
927 Saïdi, F., Ben Ismaïl, M.H., M'Rabat, A., 1997. Le Turonien de Tunisie centro-occidentale:
928 facies, paléogéographie séquentielle d'une plate-form. Cretaceous Research 18, 63–85.
929 Sarmiento, J.L., Herbert, T.D., Toggweiler, J.R., 1988. Causes of anoxia in the world ocean.
930 Global Biogechemical Cycles 2, 115–128.
931 Schlanger, S.O., Jenkyns, H.C., 1976. Cretaceous oceanic anoxic events, causes and
932 consequences. Geologie en Mijnbouw 55, 179–184.
933 Schlanger, S.O., Arthur, M.A., Jenkyns, H.C., Scholle, P.A., 1987. The Cenomanian-Turonian
934 oceanic anoxic event, I. Stratigraphy and distribution of organic-rich beds and the marine
935 $\delta^{13}C$ excursión. In: Brooks, J., Fleet, A.J. (eds.), Marine Petroleum Source Rocks. Special
936 Publication, Geol. Soc. London 26, 371–399.
937 Scholle, P.A., Arthur, M.A., 1980. Carbon isotope fluctuations in Cretaceous pelagic
938 limestones: potential stratigraphic and petroleum exploration tool. AAPG Bulletin 64, 67–
939 87.
940 Scopelliti, G., Bellanca, A., Coccioni, R., Luciani, V., Neri, R., Baudin, F., Chiari, M.,
941 Marcucci, M., 2004. High-resolution geochemical and biotic records of the Tethyan
942 'Bonarelli Level' (OAE2, latest Cenomanian) from the Calabianca-Guidaloca composite
943 section, northwestern Sicily, Italy. Palaeogeography, Palaeoclimatology, Palaeoecology
944 208, 293–317.
945 Scott, R.W., 2003. High resolution North African Cretaceous stratigraphy: status. In: Gili, E.,
946 Negra, M.H., Skelton, W. (Eds.), Cretaceous carbonate platform systems. Nato Science
947 Series 28, 1–17.
948 Sen, A.K., Filippelli, G.M., Flores, J.A., 2008. An application of wavelet analysis to
949 palaeoproductivity records from the Southern Ocean. Computers & Geosciences 35, 1445–
950 1450.

951 Sliter, W.V., 1975. Foraminiferal life and residue assemblages from Cretaceous slope deposits.
952 Geological Society of America Bulletin 86, 897–906.
953 Soua, M., Zaghbib-Turki, D., Ben Jemia, H., Smaoui, J., Boukadi, A., 2011. Geochemical
954 Record of the Cenomanian-Turonian Anoxic Event in Tunisia: Is it Correlative and
955 Isochronous to the Biotic Signal? Acta Geologica Sinica 85, 801–840.
956 Sprong, J., Kouwenhoven, T.J., Bornemann, A., Dupuis, C., Speijer, R.P., Stassen, P.,
957 Steurbaut, E., 2013. In search of the Latest Danian Event in a paleobathymetric transect off
958 Kasserine Island, north-central Tunisia. Palaeogeography Palaeoclimatology Palaeoecology
959 379, 1–-16.
960 Su, W., Wang, Y., Cramer, B.D., Munnecke, A., Li, Z., Fu, L., 2008. Preliminary estimation of
961 palaeoproductivity via TOC and habitat types: which method is more reliable? A case
962 study on the Ordovician/Silurian transitional black shales of the Upper Yangtze Platform,
963 South China. Journal of China University of Geosciences 19, 534–548.
964 Sun, Y.B., Wu, F., Clemens, S.C., Oppo, D.W., 2008. Processes controlling the geochemical
965 composition of the South China Sea sediments during the last climatic cycle. Chemical
966 Geology 257, 234–249.
967 Thierry, J., 2000. Middle Callovian (157–155 Ma). In: Dercourt, J., Gaetani, M., Vrielynck, B.,
968 Barrier, E., Biju-Duval, B., Brunet, M-F., Cadet, J.P., Crasquin, S., Sandulescu, M. (Eds.),
969 Atlas Peri-Tethys palaeogeographical maps. CCGM/CGMW, Paris, pp. 71–97.
970 Tribovillard, N., Algeo, T., Lyons, T., Riboulleau, A., 2006. Trace metals as palaeoredox and
971 palaeoproductivity proxies: an update. Chemical Geology 232, 12–32.
972 Trivobillard, N., Algeo, T.J., Baudin, F., Riboulleau, A., 2012. Analysis of marine
973 environmental conditions based on molybdenum-uranium covariation – Applications to
974 Mesozoic paleoceanography. Chemical Geology 324–325, 46–58.
975 Tsandev, I., Slomp, C.P., 2009. Modeling phosphorous cycling and carbon burial during
976 Cretaceous Oceanic Anoxic Events. Earth and Planetary Science Letters 286, 71–79.

977 Turgeon, S.C., Brumsack, H.J., 2006. Anoxic vs dysoxic events reflected in sediment
978 geochemistry during the Cenomanian-Turonian Boundary Event (Cretaceous) in the
979 Umbria-Marche basin of central Italy. Chemical Geology 234, 321–339.
980 Turgeon, S.C., Creaser, R.A., 2008. Cretaceous oceanic anoxic event 2 triggered by a massive
981 magmatic episode. Nature 454, 323–326.
982 Tyszka, J., 1994. Response of Middle Jurassic benthic foraminiferal morphogroups to
983 dysoxic/anoxic conditions in the Pieniny Klippen Basin, Polish Carpathians.
984 Palaeogeography, Palaeoclimatology, Palaeoecology 110, 55–81.
985 Valentine, J.W., 1973. Evolutionary ecology of the marine biosphere. Prentice Hall, Englewood
986 NJ, 511 pp.
987 Van Cappellen, P., Ingall, E.D., 1994. Benthic phosphorus regeneration, net primary production,
988 and ocean anoxia—A model of the coupled marine biogeochemical cycles of carbon and
989 phosphorus. Paleoceanography 9, 677–692.
990 Van der Zwaan, G.J., Duijnstee, I.A.P., Den Dulk, M., Ernst, S.R., Jannink N.T., Kouwenhoven,
991 T.J., 1999. Benthic foraminifers: proxies or problem? A review of paleoecological
992 concepts. Earth-Science Reviews 46, 213–236.
993 Wagner, T., Wallmann, K., Herrle, J.O., Hofmann, P., Stuesser, L., 2007. Consequences of
994 moderate 25,000 yr lasting emission of light CO2 into the mid-Cretaceous ocean. Earth
995 Planetary Science Letters 259, 200–211.
996 Wang, C.S., Hu, X.M., Jansa, L., Wan, X.Q., Tao, R., 2001. The Cenomanian-Turonian anoxic
997 event in southern Tibet. Cretaceous Research 22, 481–490.
998 Widmark, J.G.V., Speijer, R.P., 1997. Benthic foraminiferal faunas and trophic regimes at the
999 terminal Cretaceous Tethyan seafloor. Palaios 12, 354–371.
1000 Wignall, P.B., Myers, K.J., 1988. Interpreting the benthic oxygen levels in mudrocks: a new
1001 approach. Geology 16, 452–455.

1002 Zaghbib-Turki, D., Soua, M., 2013. High resolution biostratigraphy of the Cenomanian-
1003 Turonian interval (OAE2) based on planktonic foraminiferal bioevents in North-Central
1004 Tunisia. Journal of African Earth Sciences 78, 97–108.
1005 Zagrarni, M.F., Negra, M.H., Hanini, A., 2008. Cenomanian-Turonian facies and sequence
1006 stratigraphy, Bahloul Formation, Tunisia. Sedimentary Geology 204, 18–35.
1007 Zheng, X.Y., Jenkyns, H.C., Gale, A.S., Ward, D.J., Henderson, G.M., 2013. Changing ocean
1008 circulation and hydrothermal inputs during Ocean Anoxic Event 2 (Cenomaian-Turonian):
1009 Evidence from Nd-isotopes in the European shelf sea. Earth and Planetary Science Letters
1010 375, 338–348.
1011 Zhou, L., Wignall, P.B., Su, J., Feng, Q., Xie, S., Zhao, L., Huang, J., 2012. U/Mo ratios and
1012 $\delta^{98/95}$Mo as local and global redox proxies during mass extinction events. Chemical
1013 Geology 324-325, 99–197.
1014

1015 **Appendix 1: Planktic foraminiferal species**

1016 *Anaticinella multiloculata* (Morrow, 1934)
1017 *Dicarinella algeriana* (Caron, 1966)
1018 *Dicarinella hagni* (Scheibnerova, 1962)
1019 *Dicarinella imbricata* (Mornod, 1950)
1020 *Globigerinelloides bentonensis* (Morrow, 1934)
1021 *Globigerinelloides ultramicrus* (Subbotina, 1949)
1022 *Globoheterohelix paraglobulosa* Georgescu and Huber, 2009
1023 *Guembelitria cenomana* (Keller, 1935)
1024 *Hedbergella delrioensis* (Carsey, 1926)
1025 *Hedbergella planispira* (Tappan, 1940)
1026 *Hedbergella simplex* (Morrow, 1934)
1027 *Helvetoglobotruncana helvetica* (Bolli, 1945)
1028 *Helvetoglobotruncana praehelvetica* (Trujillo, 1960)

Heterohelix moremani (Cushman, 1938)

Heterohelix pulchra (Brotzen, 1936)

Heterohelix reussi (Cushman, 1938)

Praeglobotruncana gibba Klaus, 1960

Praeglobotruncana stephani (Gandolfi, 1942)

Rotalipora cushmani (Morrow, 1934)

Rotalipora monsalvensis (Mornod, 1950)

Shackoina bicornis (Reichel, 1948)

Schackoina cenomana (Shacko, 1897)

Thalmanninella brotzeni (Sigal, 1948)

Thalmanninella greenhornensis (Morrow, 1934)

Whiteinella aprica (Loeblich and Tappan, 1961)

Whiteinella archaeocretacea Pesaggno, 1967

Whiteinella aumalensis (Sigal, 1952)

Whiteinella baltica Douglas and Rankin, 1969

Whiteinella brittonensis (Loeblich and Tappan, 1961)

Whiteinella paradubia (Sigal, 1952)

Whiteinella sp.

Appendix 2: Benthic foraminiferal species

Ammodiscus spp.

Arenobulimina spp.

Astacolus spp.

Bathysiphon spp.

Bigenerina sp.

Bolivina sp.

Bolivinopsis sp.

Brunsvigella thoerensis (Bartenstein and Brand, 1951)

Charltonina australis Scheibnerová, 1978

Charltonina sp.

Conorotalites sp.

Coryphostoma spp.

Dorothia pupa (Reuss, 1860)

Dorothia spp.

Frondicularia sp.

Gaudryina pyramidata Cushman, 1926

Gaudryina spp.

Gavelinella barremiana Bettenstaedt, 1952

Gavelinella cenomanica (Brotzen, 1945)

Gavelinella flandrini Moullade. 1960

Gavelinella intermedia (Berthelin, 1880)

Gavelinella rochardensis Beckmann, 1991

Gavelinella spp.

Glandulina sp.

Globorotalites sp.

Globulina spp.

Gyroidinoides beisseli (White, 1928)

Gyroidinoides globosus (Hagenow, 1842)

Gyroidinoides lenticulus (Reuss, 1845)

Gyroidinoides spp.

Gyroidinoides subglobosus Dailey, 1970

Laevidentalina spp.

Lagena spp.

Lenticulina gaultina (Berthelin, 1880)

Lenticulina spp.

Lenticulina subgaultina Bartenstein, 1962

Lingulina sp.

Lingulina taylorana Cushman, 1938

Lingulogavelinella frankei (Bykova, 1953)

Lingulogavelinella sp.

Marssonella oxycona (Reuss, 1860)

Neobulimina albertensis (Stelck and Wall, 1954)

Neobulimina irregularis Cushman and Parker, 1936

Neobulimina spp.

Neobulimina subregularis (de Klasz, Magné and Rérat, 1963)

Neoflabellina sp.

Palmula sp.

Planularia advena Cushman and Jarvis, 1932

Planularia dissona Plummer, 1931

Planularia sp.

Praebulimina cf. *exigua* Cushman and Parker, 1935

Praebulimina nannina (Tappan, 1940)

Praebulimina reussi (Morrow, 1934)

Praebulimina spp.

Pyrulina spp.

Pyrulinoides spp.

Quadrimorphina sp.

Quasispiroplectammina spp.

Ramulina spp.

Reophax sp.

Repmanina charoides (Jones and Parker, 1860)

1110 *Saracenaria* sp.

1111 *Spiroplectammina* sp.

1112 *Stensioeina exsculpta* (Reuss, 1860)

1113 *Tappanina laciniosa* Eicher and Worstell, 1970

1114 *Tappanina* sp.

1115 *Textularia* sp.

1116 *Trochammina globolaevigata* Beckmann, 1991

1117 *Vaginulina* sp.

1118 *Valvulineria* sp.

1119

1120

1121

1122 **Figure caption.**

1123

1124 **Fig. 1.** (A) Geological setting, (B) palaeogeographic reconstruction of Western Tethys after
1125 Thierry (2000) and (C) Oued Bahloul section. Ammonite biostratigraphy according to
1126 Caron et al. (1999, 2006), Accarie et al. (2000), Amédro et al. (2005) and Zagrarni et al.
1127 (2008).

1128 **Fig. 2.** Planktic foraminiferal species in the Oued Bahloul section: **1-** *Globigerinelloides*
1129 *bentonensis* (OB-3.5). **2-** *Globoheterohelix paraglobulosa* (OB-42). **3-** *Guembelitria*
1130 *cenomana* (OB-24). **4-** *Hedbergella delrioensis* (OB-42). **5-** *Hedbergella planispira* (OB-
1131 22). **6-** *Hedbergella simplex* (OB-3). **7-8** *Helvetoglobotruncana helvetica* (7: OB-44, 8: OB-
1132 35). **9-** *Heterohelix moremani* (OB-13). **10-** *Heterohelix reussi* (OB-22). **11-**
1133 *Praeglobotruncana gibba* (OB-3). **12-** *Praeglobotruncana stephani* (OB-3.5). **13-**
1134 *Rotalipora cushmani* (OB-3). **14-** *Rotalipora brotzeni* (OB-3.5). **15-** *Rotalipora*
1135 *greenhornensis* (OB-3.5). **16-** *Whiteinella archaeocretacea* (OB-20). **17-** *Whiteinella aprica*
1136 (OB-37). **18** *Whiteinella brittonensis* (OB-28). Scale bars: 0.1 mm.

Fig. 3. Benthic foraminiferal species in the Oued Bahloul section: **1-** *Neobulimina albertensis* (OB-10). **2-** *Neobulimina subregularis* (OB-10). **3-** *Praebulimina prolixa* (OB-24). **4-** *Lenticulina gaultina* (OB-2). **5-** *Gyroidinoides lenticulus* (OB-2). **6-** *Gyroidinoides globosus* (OB-2). **7-** *Praebulimina nannina* (OB-2). **8-** *Gaudryina pyramidata* (OB-3). **9-** *Marssonella oxycona* (OB-3). **10-** *Lenticulina* sp (OB-3). **11-** *Trochammina globolaevigata* (OB-3). **12-** *Praebulimina* sp (OB-8). **13-** *Praebulimina reussi* (OB-8). **14-** *Gavelinella rochardensis* (OB-8). **15-** *Planularia advena* (OB-35.5). **16-***Tappanina laciniosa* (OB-33). **17-** *Gavelinella* cf. *rochardensis* (OB-22). **18-** *Astacolus* ? sp. (OB-35). Scale bars: 0.1 mm

Fig. 4. Stratigraphic distribution of planktic/benthic ratio and diversity of planktic and benthic foraminifera.

Fig. 5. Stratigraphic distribution of planktic foraminiferal assemblages.

Fig. 6. Stratigraphic distribution of benthic foraminiferal assemblages.

Fig. 7. Stratigraphic fluctuations of geochemical redox proxies and U- and Mo-based proxies (enrichment factor and authigenic content).

Fig. 8. Stratigraphic fluctuations of CO_3Ca content, TOC and geochemical palaeproductivity proxies.

Fig. 9. Stratigraphic fluctuations of $\delta^{13}C$ and $\delta^{18}O$ and comparison with previous $\delta^{13}C$ curves of Caron et al. (2006) (dashed line) and Zagrarni et al. (2008) (dotted line).

Fig. 10. Evolution of trophic conditions, productivity and oxygenation in the water column and the seafloor (sea-bottom waters) inferred from foraminiferal assemblages and geochemical proxies.

Table caption

Table 1. Planktic foraminiferal counts per sampling level.

Table 2. Benthic foraminiferal counts per sampling level.

1163 Table 3. Planktic forms and inferred life style including redox and trophic requirements of
1164 planktic foraminifera from Ouled Bahloul section based on Hart and Bailey (1979), Hart
1165 (1999), Keller et al. (2001) and Coccioni and Luciani (2005).

Figure 01
Click here to download high resolution image

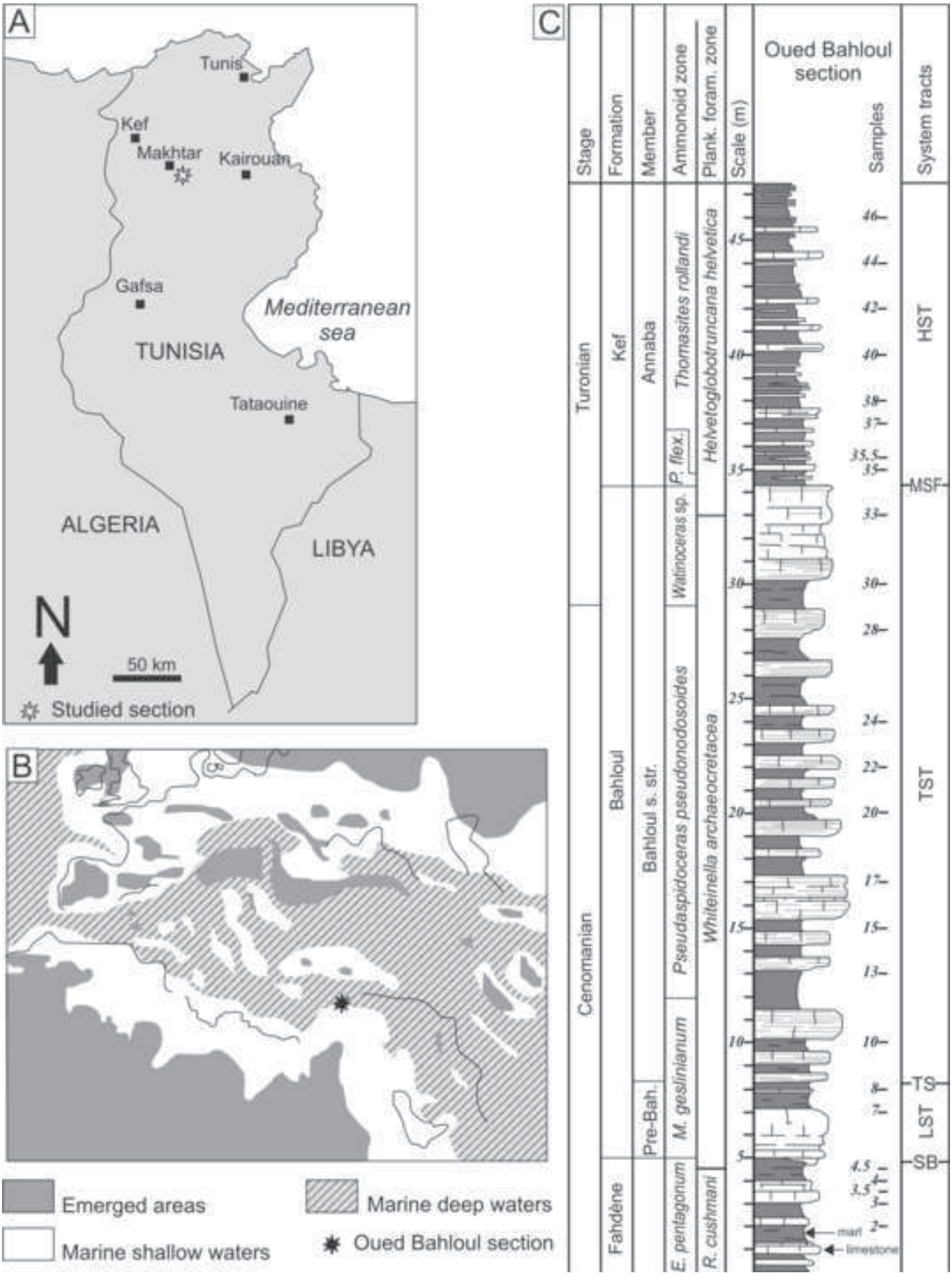

Figure 02
Click here to download high resolution image

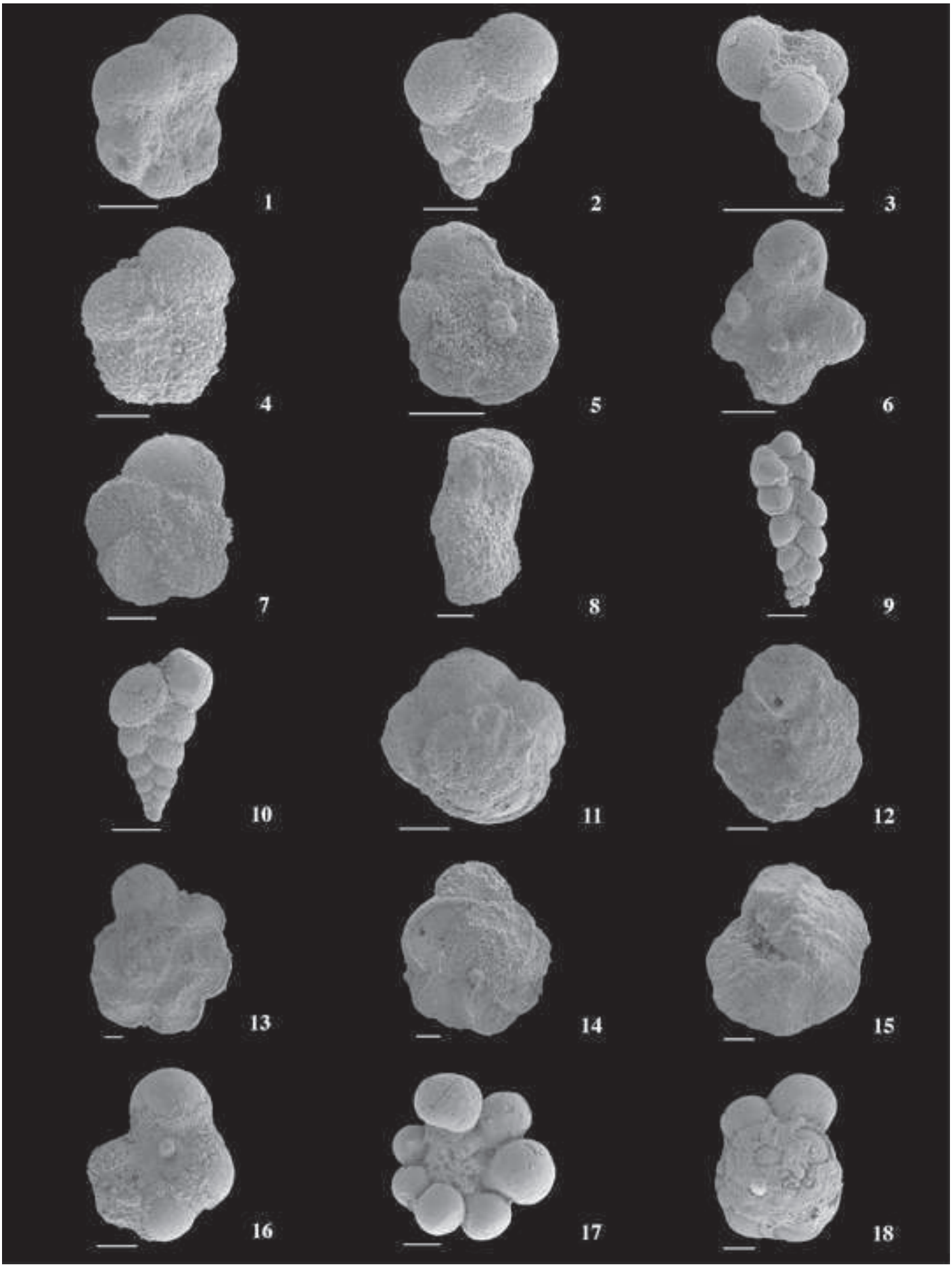

Figure 03
Click here to download high resolution image

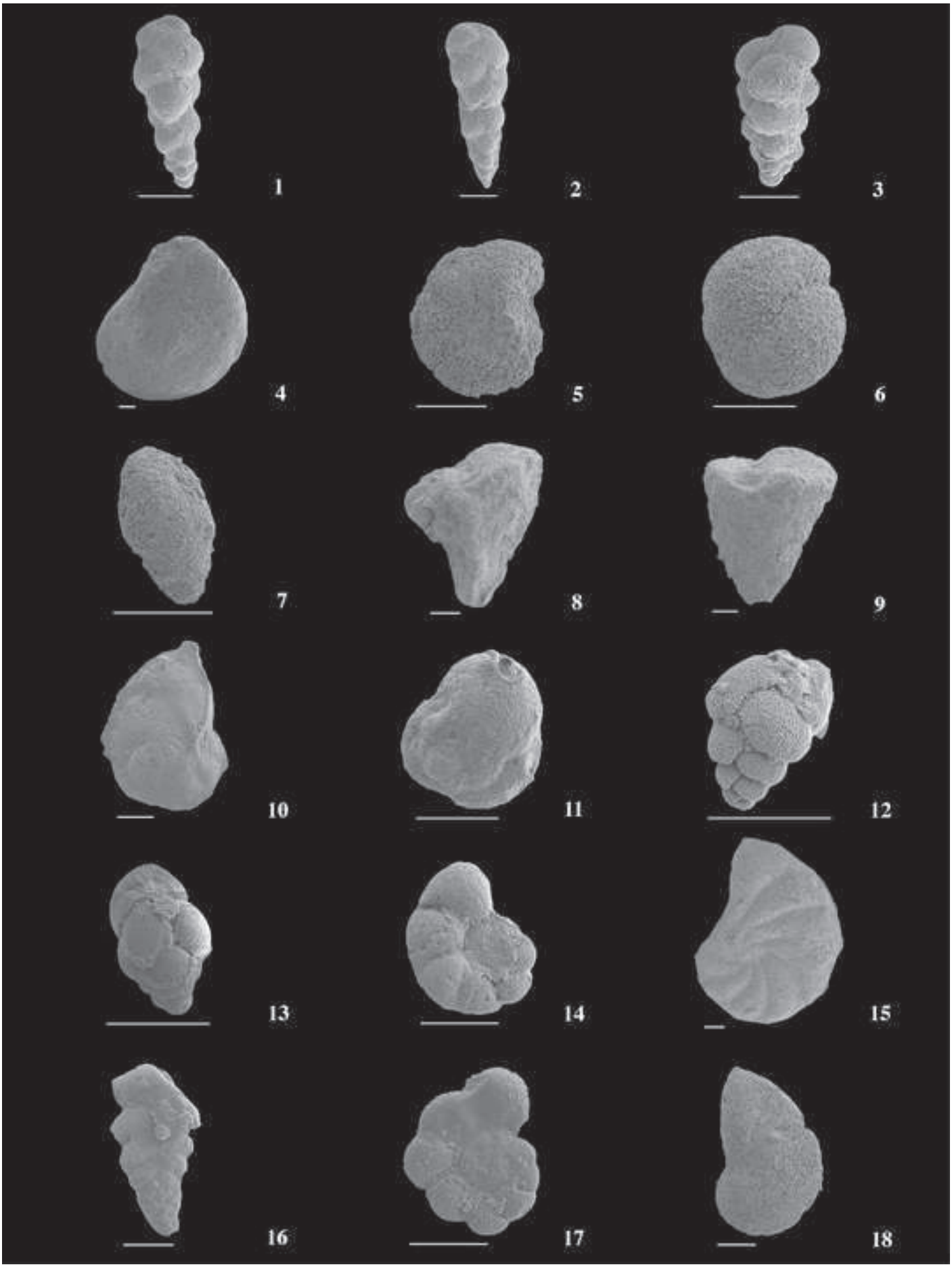

Figure 04
Click here to download high resolution image

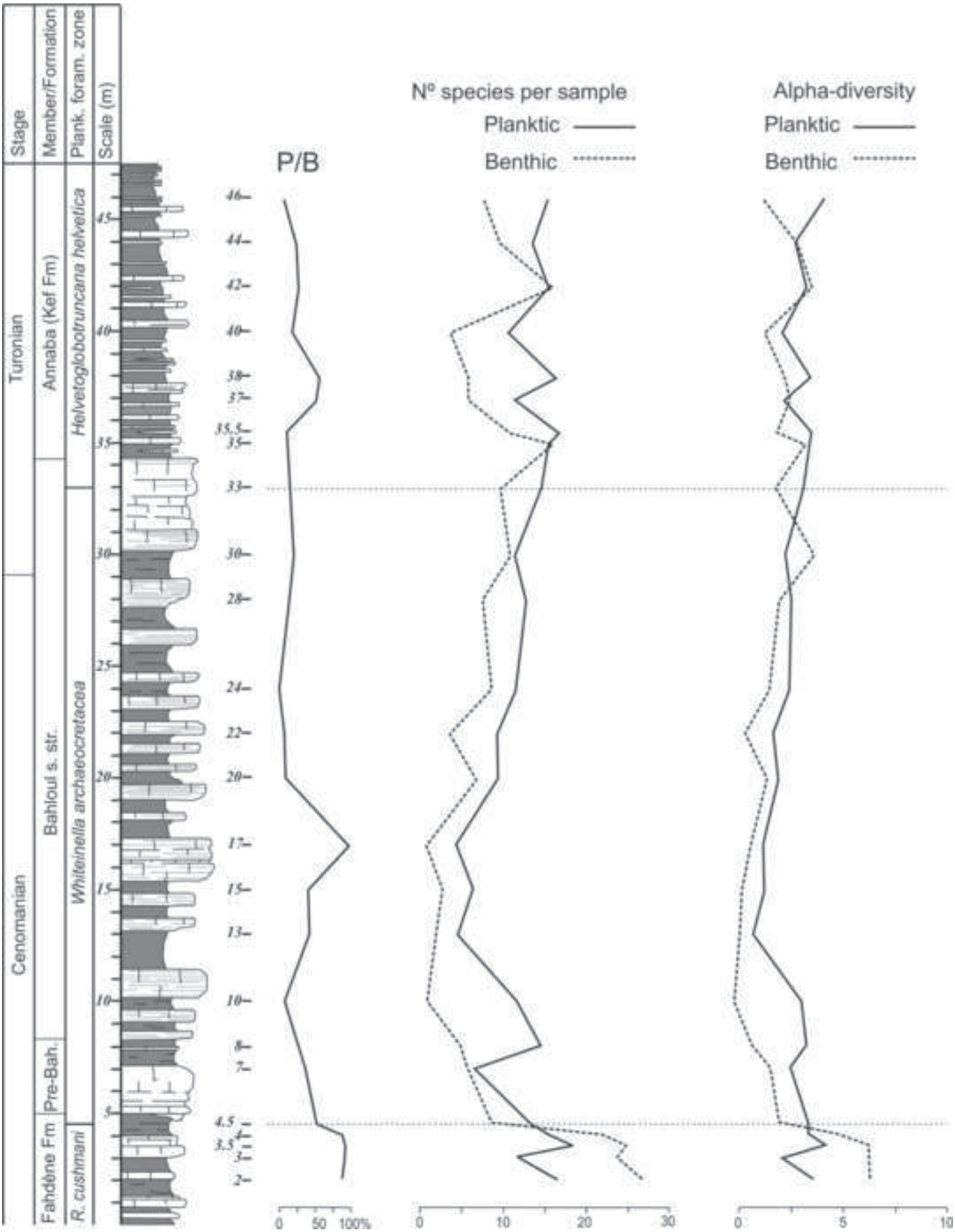

Figure 05

Click here to download high resolution image

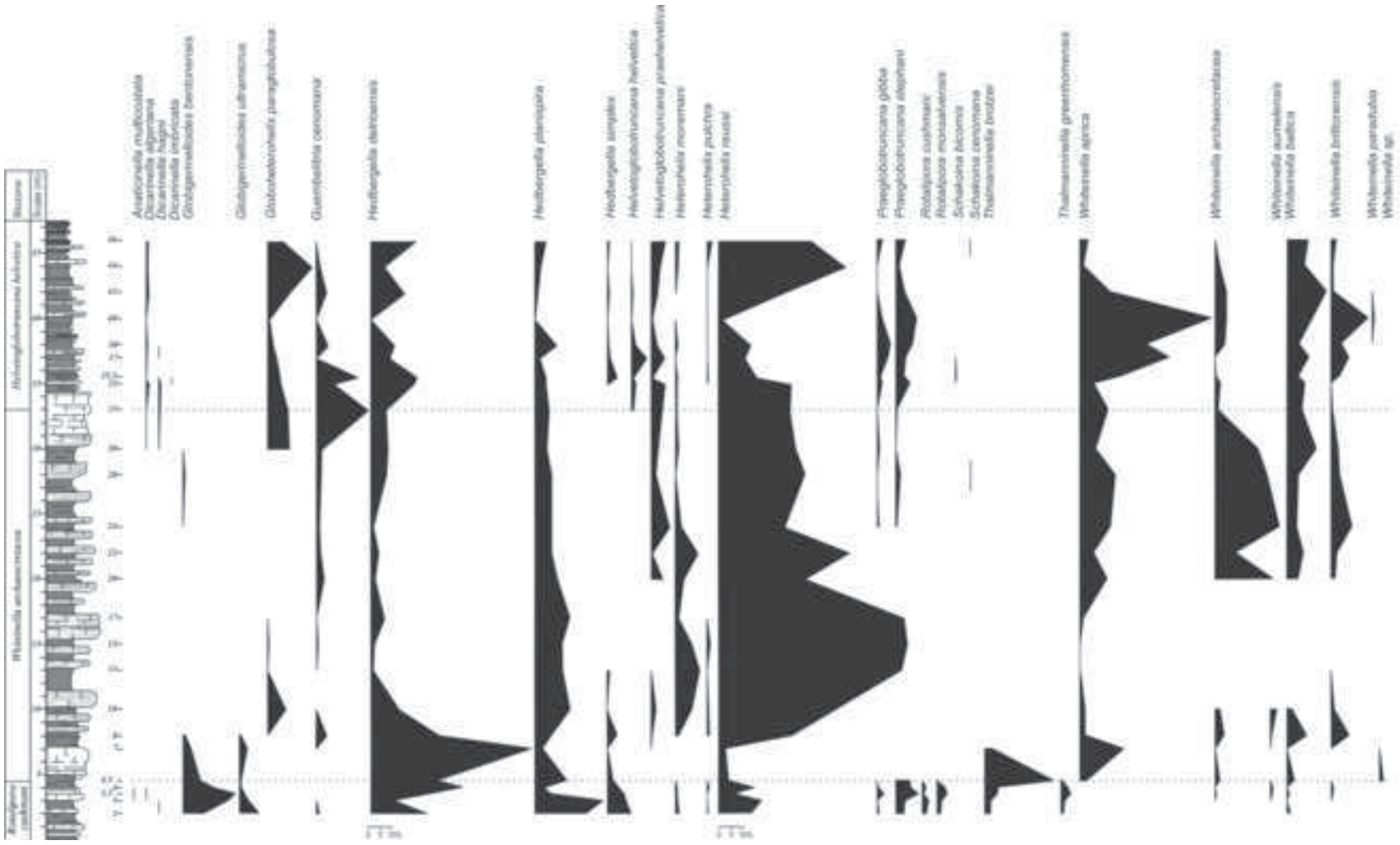

Figure 06a

Click here to download high resolution image

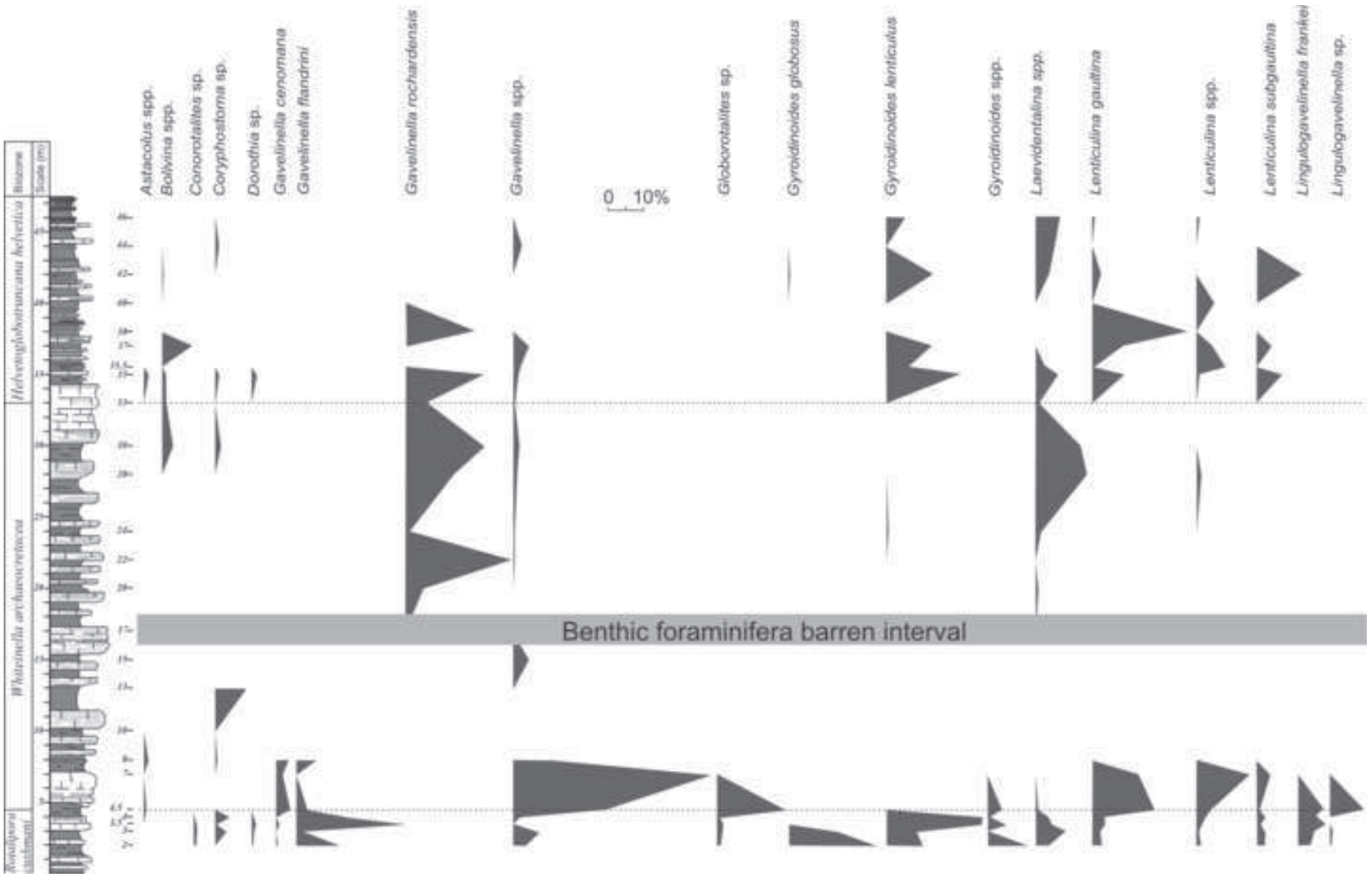

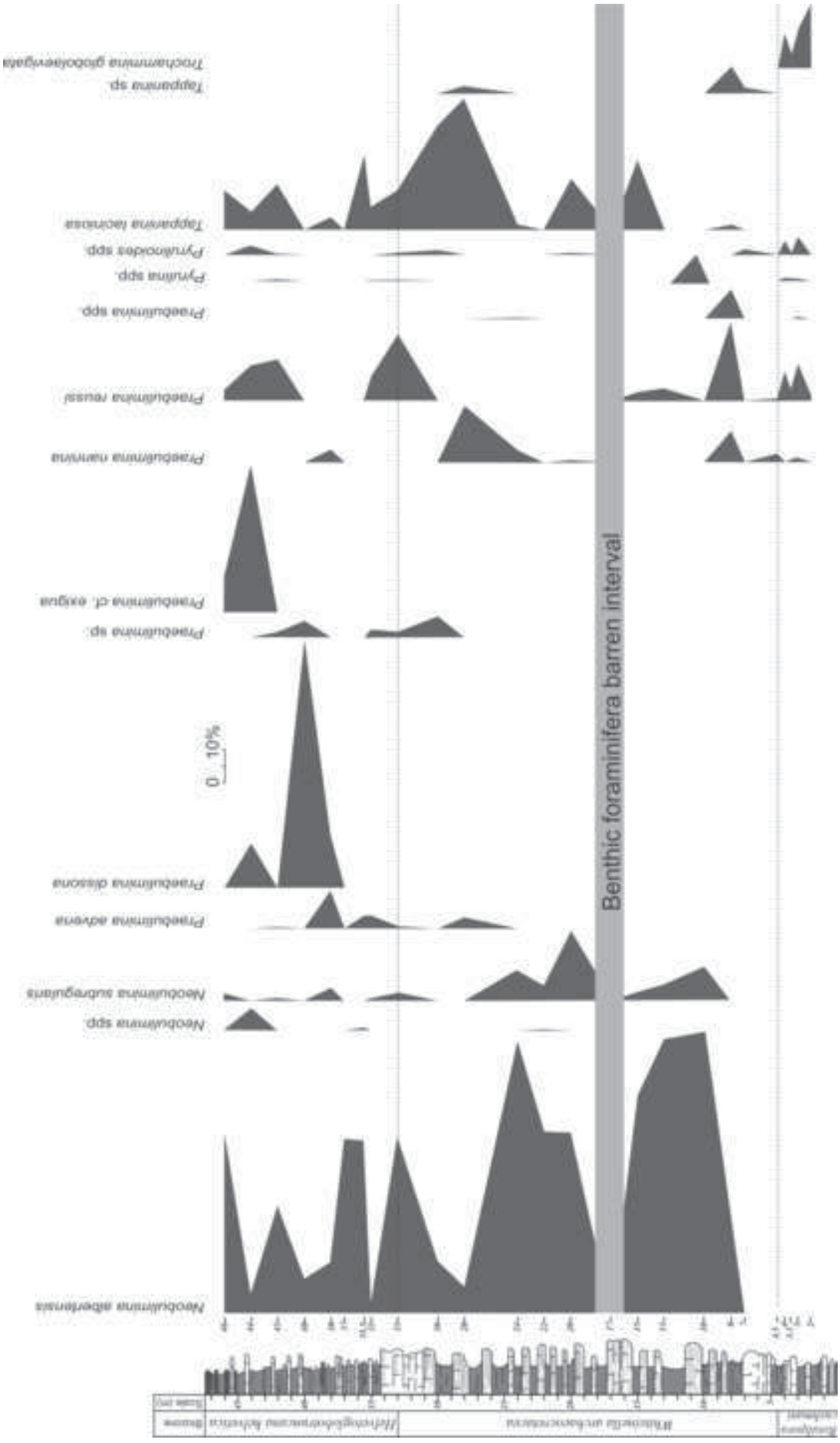

Figure 06b
Click here to download high resolution image

Figure 07

Click here to download high resolution image

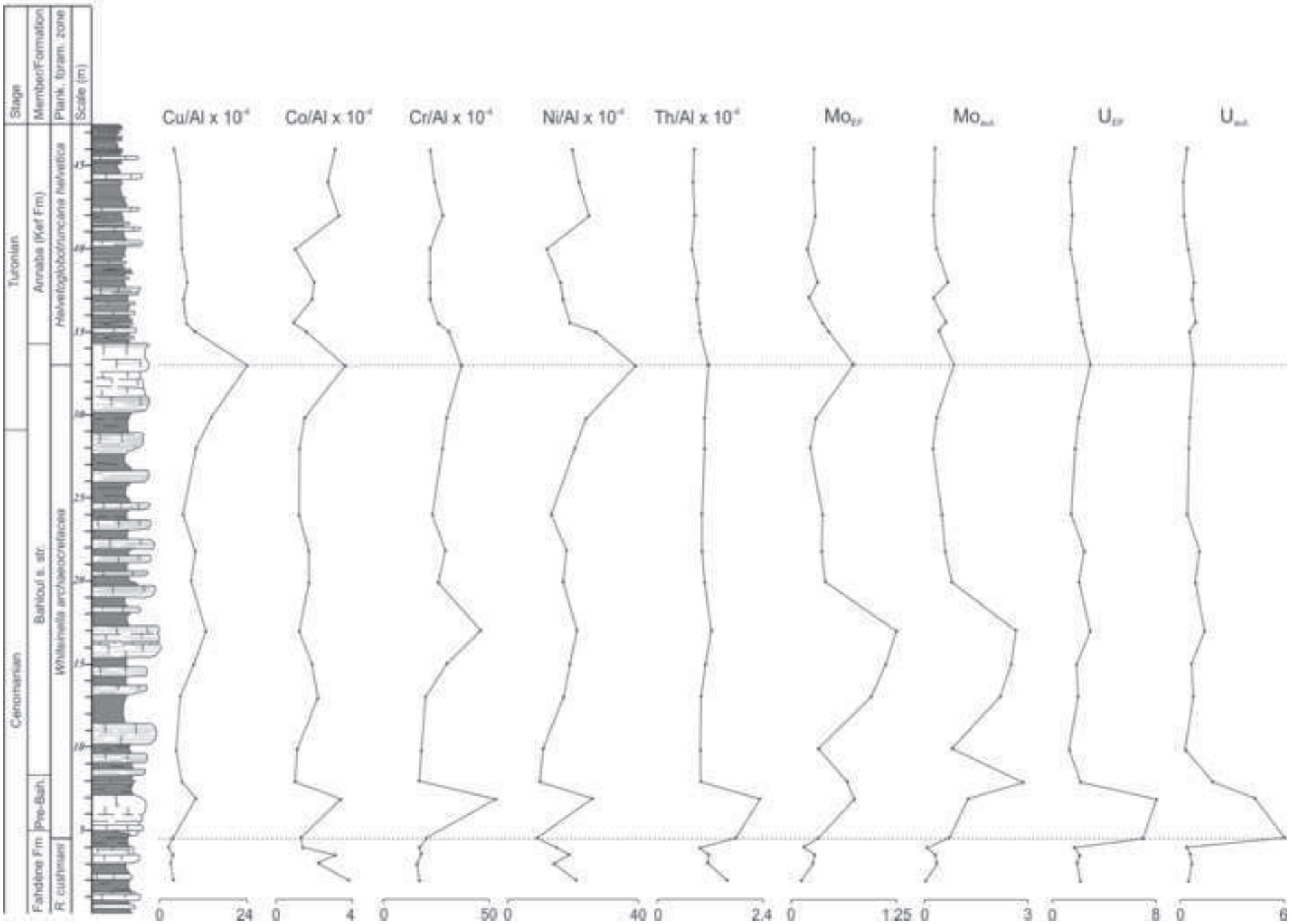

Figure 08

Click here to download high resolution image

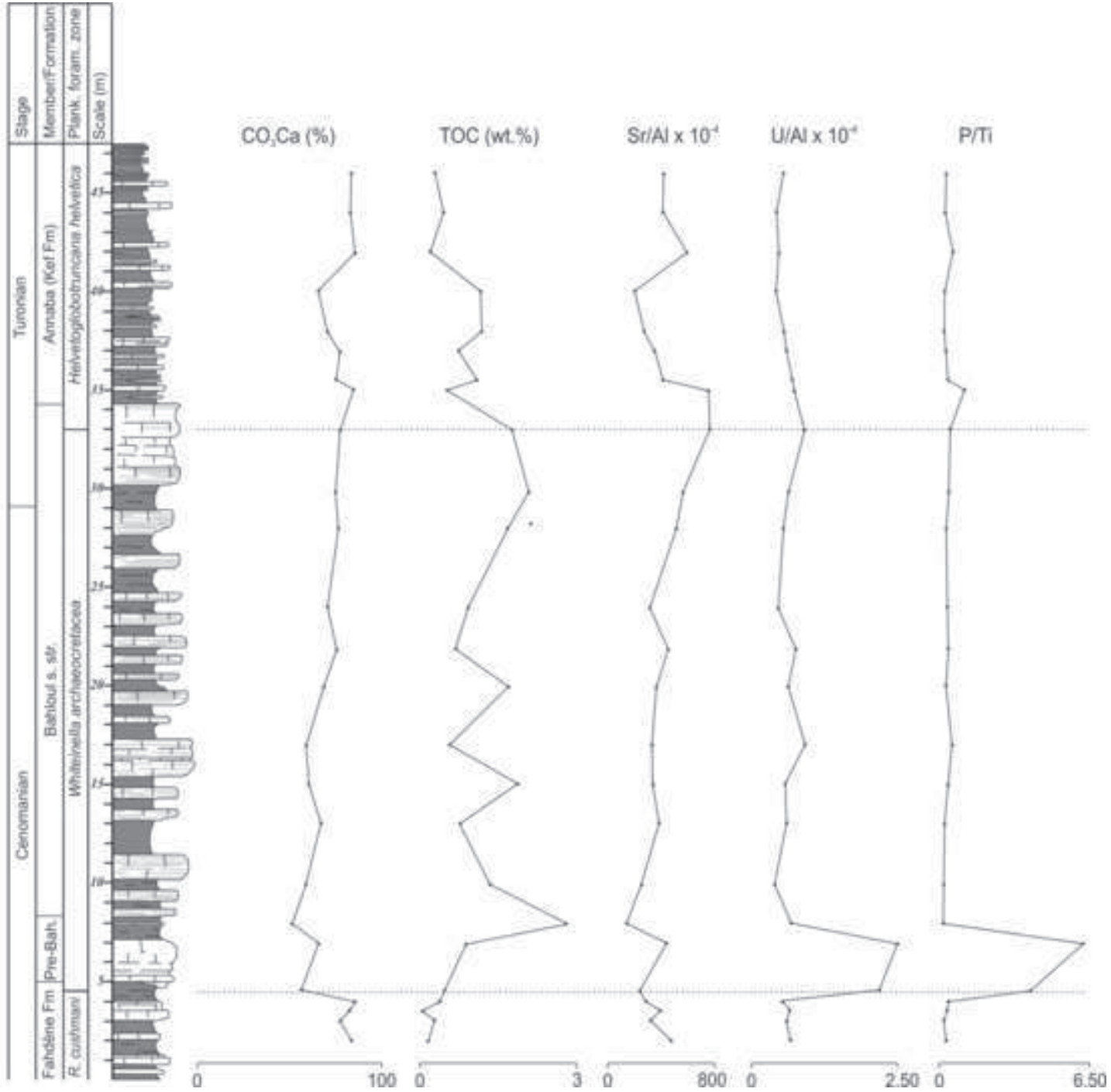

Figure 09
Click here to download high resolution image

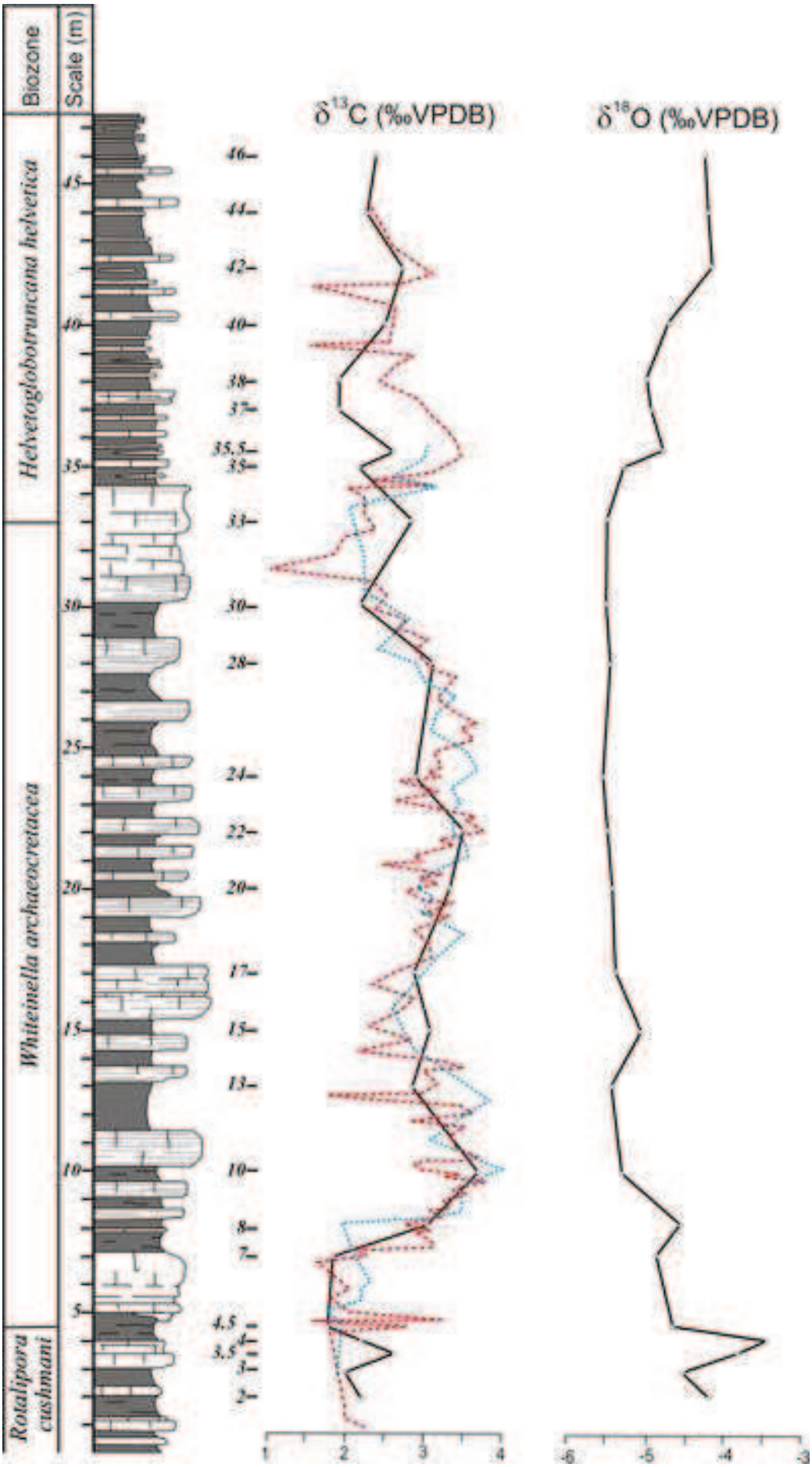

Figure 10

Click here to download high resolution image

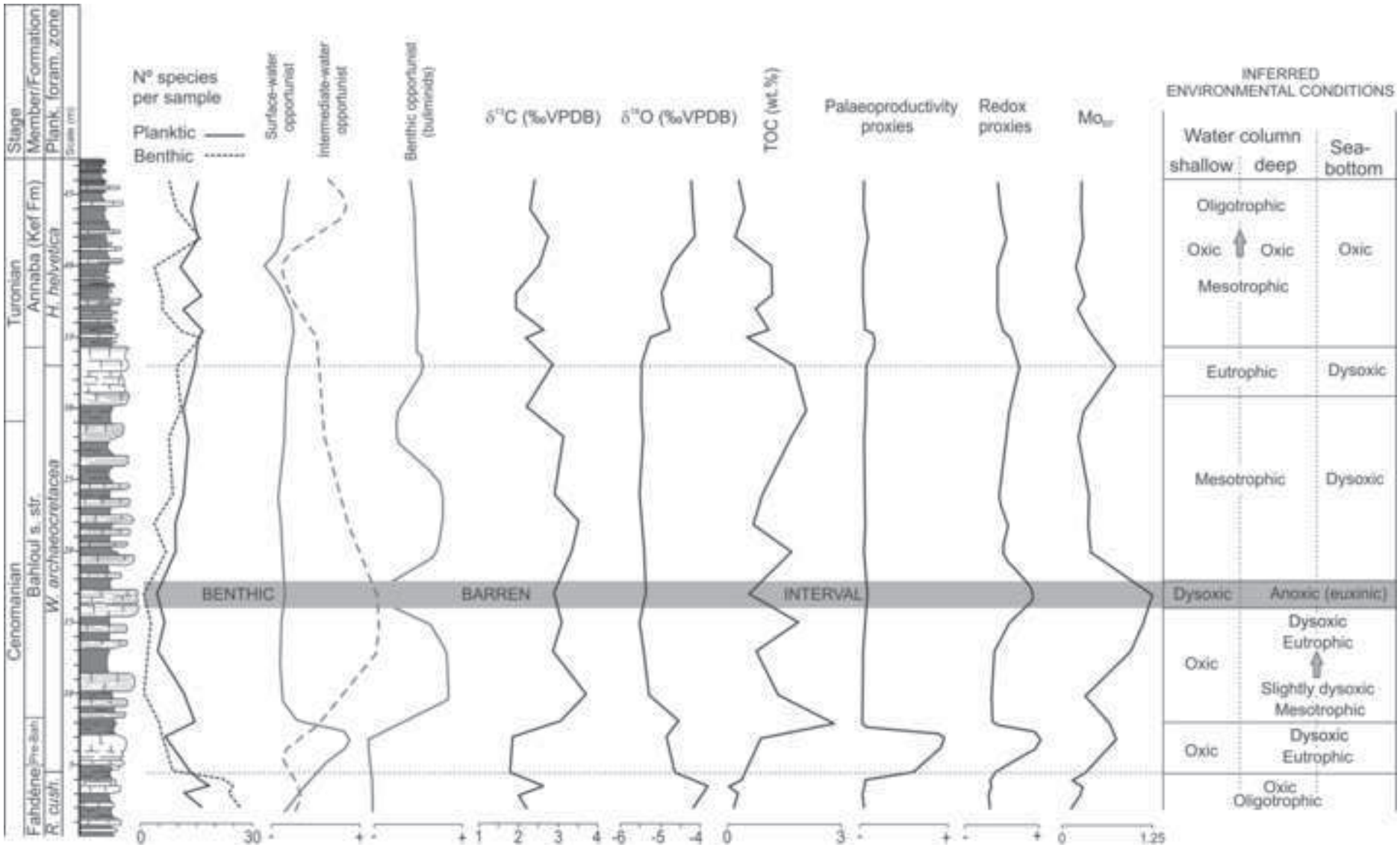

Table 01
Click here to download Table: Table 1.xlsx

SAMPLE \ SPECIES	*Anaticinella multiloculata*	*Dicarinella algeriana*	*Dicarinella hagni*	*Dicarinella imbricata*	*Globigerinelloides bentonensis*	*Globigerinelloides ultramicrus*	*Globoheterohelix paraglobulosa*	*Guembelitria cenomana*	*Hedbergella delrioensis*	*Hedbergella planispira*	*Hedbergella simplex*	*Helvetoglobotruncana helvetica*	*Helvetoglobotruncana praehelvetica*	*Heterohelix moremani*
OB10-46	0	4	0	0	0	0	26	0	82	19	4	1	26	6
OB10-44	0	3	0	0	0	0	66	6	19	8	1	0	13	4
OB10-42	0	5	0	0	0	0	37	17	57	5	3	3	11	0
OB10-40	0	0	0	0	0	0	3	0	0	0	0	1	2	0
OB10-38	0	3	1	0	0	0	10	21	41	38	3	8	11	4
OB10-37	0	0	0	0	0	0	15	0	31	7	5	25	22	0
OB10-35.5	0	0	0	0	0	0	20	68	73	17	17	3	2	4
OB10-35	0	5	3	1	0	0	19	25	61	15	0	7	20	3
OB10-33	0	1	2	0	0	0	27	70	21	19	0	3	15	2
OB10-30	0	0	0	0	0	0	32	8	25	17	0	0	10	5
OB10-28	0	0	0	0	2	0	0	7	22	23	0	0	7	1
OB10-24	0	0	0	0	0	0	0	4	4	20	0	0	23	8
OB10-22	0	0	0	0	0	0	0	7	14	27	0	0	2	38
OB10-20	0	0	0	0	0	0	0	12	7	35	0	0	18	13
OB10-17	0	0	0	0	0	0	0	0	4	10	0	0	0	1
OB10-15	0	0	0	0	0	0	1	2	4	30	0	0	0	18
OB10-13	0	0	0	0	0	0	0	0	4	40	4	0	0	35
OB10-10	0	0	0	0	0	0	11	0	17	21	0	0	3	10
OB10-8	0	0	0	0	3	2	0	14	89	22	12	0	1	4
OB10-7	0	0	0	0	1	1	0	0	22	1	0	0	0	0
OB10-4.5	0	0	0	0	14	1	0	0	57	27	5	0	0	0
OB10-4	0	0	0	0	47	3	0	0	143	12	17	0	0	3
OB10-3.5	1	1	0	0	78	8	0	0	90	25	25	0	0	3
OB10-3	0	0	0	0	80	16	0	0	42	123	34	0	0	5
OB10-2	0	0	1	0	32	31	0	5	89	80	38	0	0	6

Table 02
Click here to download Table: Table 2.xlsx

SAMPLE \ SPECIES	*Ammodiscus* spp.	*Arenobulimina* spp.	*Astacolus* spp.	*Bathysiphon* spp.	*Bigenerina* sp.	*Bolivina* sp.	*Bolivinopsis* sp.	*Brunsvigella thoerensis*	*Charltonina australis*	*Charltonina* sp.	*Conorotalites* sp.	*Coryphostoma* spp.	*Dorothia pupa*	*Dorothia* spp.	*Frondicularia* sp.	*Gaudryina pyramidata*
OB10-46	0	0	0	0	0	0	0	0	0	0	0	0	0	0	1	0
OB10-44	0	0	0	0	0	0	0	0	0	0	0	1	0	0	0	0
OB10-42	0	1	0	0	0	1	0	0	0	0	0	0	0	0	0	0
OB10-40	0	0	0	0	0	0	0	0	0	0	0	0	0	0	0	0
OB10-38	0	0	0	0	0	0	0	0	0	0	0	0	0	0	0	0
OB10-37	0	0	0	0	0	2	0	0	0	0	0	0	0	0	0	0
OB10-35.5	0	0	0	0	0	0	0	0	0	0	0	0	0	0	0	0
OB10-35	0	0	5	0	0	4	0	0	0	0	0	4	0	6	2	0
OB10-33	0	0	0	1	0	3	0	0	0	0	0	0	0	0	0	0
OB10-30	0	0	0	0	0	2	0	0	0	0	0	1	0	0	0	0
OB10-28	0	0	0	0	0	0	0	0	0	0	0	0	0	0	0	0
OB10-24	0	0	0	0	1	0	0	0	0	0	0	0	0	0	0	0
OB10-22	0	0	0	0	0	0	0	0	0	0	0	0	0	0	0	0
OB10-20	0	0	0	0	0	0	0	2	0	0	0	0	0	0	0	0
OB10-17	0	0	0	0	0	0	0	0	0	0	0	0	0	0	0	0
OB10-15	0	0	0	0	0	0	0	0	0	0	0	0	0	0	0	0
OB10-13	0	0	0	0	0	0	0	0	0	0	0	9	0	0	0	0
OB10-10	0	0	0	0	0	0	0	0	0	0	0	0	0	0	0	0
OB10-8	0	0	2	0	0	0	0	0	0	0	0	1	0	0	0	0
OB10-7	0	0	0	0	0	0	0	0	0	0	0	0	0	0	0	0
OB10-4.5	0	0	1	0	0	0	0	0	0	0	0	0	0	0	1	0
OB10-4	1	0	1	0	0	0	0	0	7	0	1	14	0	2	0	0
OB10-3.5	2	0	0	1	0	0	2	0	1	0	3	1	0	4	0	2
OB10-3	0	0	0	0	0	0	0	0	0	0	3	8	3	2	0	2
OB10-2	1	0	0	0	0	0	0	0	2	1	3	0	2	1	0	0

Table 03
Click here to download Table: Table 3.xls

Morphology	Genera	Habitat	Mode
Strongly keeled trochospiral	*Dicarinella*	Intermediate-dweller	Intermediate
	Rotalipora	Intermediate to deep-	Specialist
	Thalmanninella	Intermediate to deep-	Specialist
Weakly keeled trochospiral	*Anaticinella*	Intermediate-dweller	Intermediate
	Helvetoglobotruncana	Intermediate to deep-dweller	Intermediate to specialist
	Praeglobotruncana	Intermediate-dweller	Intermediate
Unkeeled trochospiral	*Hedbergella*	Surface-dweller	Opportunist
	Shackoina	Intermediate-dweller	Intermediate
	Whiteinella	Surface-dweller	Opportunist
Planispiral	*Globigerinelloides*	Surface to intermediate-dweller	Opportunist to Intermediate
Biserial	*Heterohelix*	Surface to intermediate -dweller	Opportunist
Triserial	*Guembelitria*	Surface-dweller	Opportunist